Coordination Chemistry Reviews xxx (2012) xxx–xxx

Contents lists available at SciVerse ScienceDirect

Coordination Chemistry Reviews

journal homepage: www.elsevier.com/locate/ccr

Review

Understanding copper-thiolate containing electron transfer centers by incorporation of unnatural amino acids and the Cu_A center into the type 1 copper protein azurin

Tiffany D. Wilson[a], Yang Yu[b], Yi Lu[a,b,*]

[a] Department of Chemistry, Urbana, IL 61801, United States
[b] Center for Biophysics and Computational Biology, Urbana, IL 61801, United States

Contents

ARTICLE INFO

Article history:
Received 5 March 2012
Received in revised form 15 June 2012
Accepted 19 June 2012
Available online xxx

Keywords:
Redox
Electron transfer
Cupredoxins
Copper proteins
Type 1 copper
Blue copper
Cu_A
Biosynthetic chemistry
Protein engineering

ABSTRACT

Highly covalent copper-thiolate bonds are salient features of ubiquitous type 1 (T1) blue copper and purple Cu_A electron transfer (ET) centers in proteins. These centers are found in a wide variety of proteins, each having its own electron transfer partners, requiring the centers to possess a broad range of reduction potentials to match those of their redox partners and to perform ET functions under various driving forces, all while maintaining high ET efficiency. Unraveling the secrets of the success realized by these ET centers has relied upon the expertise of many scientific disciplines and sub-disciplines, including inorganic chemistry, microbiology, biochemistry, and biophysical chemistry. Here, we review the contribution of protein engineering approaches—namely, the incorporation of unnatural amino acids and a biosynthetic Cu_A cofactor into the T1 copper protein azurin—to advancing the current understanding of how the unique structures of T1 copper and Cu_A centers confer their proteins with efficient and tailored ET properties.

* Corresponding author at: Department of Chemistry, University of Illinois at Urbana-Champaign, Urbana, IL 61801, United States. Tel.: +1 217 333 2619.
E-mail address: yi-lu@illinois.edu (Y. Lu).

0010-8545/$ – see front matter © 2012 Elsevier B.V. All rights reserved.
http://dx.doi.org/10.1016/j.ccr.2012.06.015

1. Introduction

Electron transfer lies at the heart of countless biological processes. Transition metals, often stable in multiple oxidation states, are well-suited to fulfill this role. While catalytic centers typically perform the actual chemical transformations from which life forms draw energy, such as oxygen [1] and nitrous oxide [2] reduction, these centers would be defunct without a steady, reliable, and rapid supply of electrons. To this end, superb electron transfer centers based upon transition metals have evolved, utilizing iron or copper. As the fields of inorganic chemistry, microbiology, biochemistry, and biophysical chemistry have burgeoned, so too has our understanding of how these electron transfer centers accomplish their task with such efficiency and elegance. This review focuses on advances made to our knowledge of copper-thiolate containing ET centers from a number of protein engineering studies, employing unnatural amino acids and an engineered Cu_A cofactor, in the type 1 (T1) copper protein, azurin (Az).

1.1. Electron transfer by copper-thiolate centers in proteins

For the purposes of this review, biological copper-based electron transfer centers fall into two classifications, depending on their geometric and spectroscopic properties: mononuclear type 1 (T1) copper and dinuclear Cu_A [3–11]. Together, these two types of ET centers are found across all domains of life. Both types of centers transfer electrons rapidly and efficiently, and both feature highly covalent copper-thiolate bonds. The presence of these Cu—S bonds combines with the paramagnetic Cu(II) oxidation state to provide a wealth of spectroscopic information about these sites, which in turn informs on their electronic and geometric structures. Immediately noticeable for those who have studied these proteins are the brilliant blue or purple colors of their solutions, arising from the Cu—S bonds, which generate intense ($\varepsilon \sim 2000$–$6000\ M^{-1}\ cm^{-1}$) ligand-to-metal charge transfer (LMCT) bands [12,13]. These bright colors have led to the use of "blue copper" for T1 copper centers and "purple copper" for Cu_A centers.

1.1.1. Blue T1 copper centers: the common currency of copper-based electron transfer

Proteins containing the T1 copper center occur ubiquitously, and have a wide range of electron transfer partners involved in a great variety of processes [3–10]. In this sense, T1 copper centers are the common currency of copper-based electron transfer in biology. However, as is discussed in this section, the properties of the T1 copper site make it anything but "common" when compared to standard aqueous copper complexes.

T1 copper proteins belong to a class called the cupredoxins, which all share a similar Greek-key β-barrel fold (Fig. 1A) [3–10,14]. Despite the functional versatility demonstrated by T1 copper centers, *i.e.* their occurrence in many proteins that transfer electrons from and to a variety of partners, the primary coordination spheres of these T1 copper centers are highly conserved. The minimum coordination set consists of three strong ligands, two δ-N His imidazolyls and one Cys thiolate, which result in a trigonal ligand arrangement about the copper ion. In the majority of T1 copper sites, a Met thioether, and in some cases, a backbone carbonyl, comprise weaker axial ligands, giving distorted tetrahedral (Met only) or distorted trigonal bipyramidal (Met and RR′—C=O) geometries (Fig. 1B) [3–10].

The strong thiolate coordination in T1 copper centers results in an intense ($\varepsilon \sim 2000$–$6000\ M^{-1}\ cm^{-1}$) LMCT band at ~600–640 nm, which has been attributed to π-overlap between the Cys-S 3p and copper $3d(x^2 - y^2)$ orbitals, as well as a typically weaker LMCT band at ~400 nm, which is due to σ-overlap of these same orbitals [8]. In cases where the axial distortion is stronger, leading to a more tetrahedral geometry, the ratio of the intensity of the 400 nm/600 nm bands increases, due to greater σ-overlap, and the resulting green color gives these special cases of T1 copper sites the name of "green copper" [15]. The strong thiolate ligation in T1 copper centers also leads to copper hyperfine splittings ($A_{||}$) less than half the size

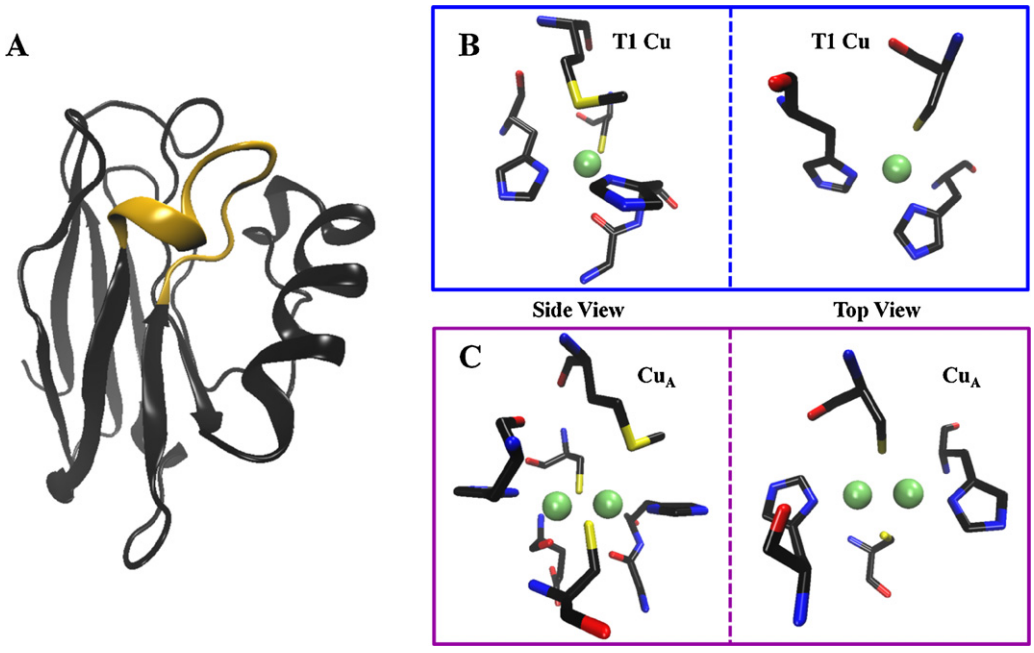

Fig. 1. (A) Greek-key β-barrel fold exhibited by T1 copper and Cu_A proteins (from apo-azurin structure, PDB ID 1E65). The ligand loop containing the majority of the copper binding residues is highlighted in gold. (B) T1 copper site of azurin (PDB ID 4AZU), showing a side view (left) and top view (right) of the center. The top view contains the minimal set of ligands (His_2Cys) required to form a T1 copper center. (C) Cu_A site of Cu_AAz (PDB ID 1CC3), showing a side view (left) and top view (right) of the center. In both (B) and (C), axial ligands are removed from the top view for clarity. Color code in (B) and (C): carbon is black, oxygen is red, nitrogen is blue, sulfur is yellow, and copper is green.

Please cite this article in press as: T.D. Wilson, et al., Coord. Chem. Rev. (2012), http://dx.doi.org/10.1016/j.ccr.2012.06.015

($\sim$40–60 $\times$ 10^{-4} cm^{-1}) of those of aqueous copper complexes in their electron paramagnetic resonance (EPR) spectra, due to delocalization of the unpaired electron to the thiolate and away from the nuclear spin of the copper [8]. The covalency of this Cu—S(Cys) bond, which dictates the spectroscopic features to such a large extent, has been quantified at $\sim$40% spin density on the Cys S-3p orbitals in the ground state [8,16].

In addition to the remarkable blue color of solutions of T1 copper proteins, it was discovered that T1 copper sites function at very high reduction potentials (up to >1 V *vs* NHE) [17], as compared to aqueous copper ions (<200 mV). Together, these two facts stirred much interest in T1 copper proteins and debate about the source of these unusual properties, dating back to the 1950s [4]. Synthetic inorganic chemists started pursuing small molecule mimics of this site, while many bioinorganic chemists carried out spectroscopic and mutagenesis studies of native T1 copper centers [7]. As spectroscopic techniques became more sophisticated and computational methods improved, molecular orbital descriptions were developed for T1 copper sites, which have been thoroughly reviewed [3–10,15]. These studies showed that the extremely efficient electron transfer of T1 copper centers, in which rapid electron transfer is facilitated across distances >10 Å, can largely be attributed to two features of this site: its unique geometry and highly covalent Cu—S bond.

Owing to advances in biomacromolecular crystallography, several crystal structures of T1 copper proteins became available in the 1990s, including many in both the reduced and oxidized states [3,4,11,14]. It was recognized from these structures that the geometry of T1 copper centers was very unusual for Cu(II) complexes. Whereas the geometry of the T1 copper centers were distorted tetrahedral or trigonal bipyramidal, the geometries of small molecule Cu(II) complexes were typically tetragonal, such as square planar, square pyramidal, and square bipyramidal. Conversely, tetrahedral and trigonal bipyramidal geometries were characteristic of small molecule Cu(I) complexes. Examination of the differences between the reduced and oxidized structures of T1 copper proteins also revealed very small geometrical changes upon reduction/oxidation of the site, suggesting that the inner sphere reorganization energy of these centers was quite small compared to aqueous copper complexes [4]. Indeed, measurements of the reorganization energy of T1 copper proteins yielded values of $\sim$0.7 eV versus the >1 eV reorganization energies of aqueous copper complexes [4,8]. A small reorganization energy contributes significantly to rapid electron transfer. Calculations have shown that $\sim$70% of the inner sphere reorganization energy of unconstrained copper complexes arises from tetragonal distortion of their geometries upon oxidation [8]. This tetragonal distortion is a required Jahn–Teller distortion, relieving orbital degeneracy that exists for Cu(II) ions placed in the geometry of the reduced state. Orbital degeneracy is not present in the asymmetric environment of T1 copper proteins, avoiding the need for Jahn–Teller distortions. Thus, the unusual geometry imposed by T1 copper proteins plays a key role in their success as rapid electron transfer agents, by greatly lowering their reorganization energies relative to aqueous copper complexes.

Another factor that is crucial to facilitating rapid, long-distance electron transfer is the electronic coupling between donor and acceptor sites [8]. High covalency in a metal–ligand bond greatly amplifies coupling between donor and acceptor metal centers. Additionally, anisotropy in the covalent character of a ligand set provides directionality to electron transfer. Correlating electronic structure calculations to spectroscopic data, Solomon and coworkers showed that the high level of anisotropic covalency due to the Cu—S(Cys) bond in one T1 copper protein, plastocyanin, allows the electron transfer pathway involving this bond to overcome an $\sim$1500$\times$ difference in rate from the much shorter electron entry path through one of the His ligands (as calculated based purely on donor–acceptor distances) [8,18]. Thus, the covalency of this Cu—S(Cys) bond determines to a large extent the electron transfer efficiency of T1 copper centers.

As shown by their unique properties, both structural and functional, T1 copper centers, the common currency of copper-based biological electron transfer, are not "common" at all, but rather, key players in extraordinary, exquisitely tuned biological wires. The picture presented in this section shows that our understanding of this center is certainly sophisticated. However, as will be discussed later in the review (Section 2), some facets of these centers still remained to be elucidated or experimentally corroborated.

1.1.2. Purple Cu_A centers: Nature's gold reserves in copper-based electron transfer

Cu_A centers crop up only in very specialized instances, at or near the termini of electron transport chains [19–28]. To date, this copper center has only been found in cytochrome *c* oxidase (C*c*O, terminus of aerobic respiration chain) [1,22,29–32], nitrous oxide reductase (N_2OR, terminus of anaerobic respiration chain) [33–35], nitric oxide reductase (NOR, near terminus of anaerobic respiration chain) [36,37] and SoxH (terminal oxidase in *Sulfolobus acidocaldarius*) [38,39]. Thus, if T1 copper centers are the common currency of copper-based electron transfer in biology, Cu_A centers are the gold reserves, to be brought out and used only for special purposes. Indeed, as will be discussed in this section and Section 3, the structural and functional properties of the Cu_A site are even more complex and peculiar than those of the T1 copper centers, and were relatively poorly understood until recently.

Cu_A centers are housed in domains or subunits of larger enzymes or enzymatic complexes, which, like T1 copper proteins, adopt Greek-key β-barrel folds (Fig. 1A) [7,9,22,29,33,34,40–42]. Unlike the T1 copper centers, Cu_A centers are dinuclear, with a completely conserved ligand set. The two copper ions are bridged by two Cys thiolates and form a direct metal–metal bond with each other, creating a rigid diamond core (Fig. 1C) [7,9,22,29,33,34,40–44]. Together with the Cys thiolates, a His δ-N imidazolyl coordinates each copper ion, generating for each a trigonal coordination environment. Weak axial ligands, a Met thioether for one copper ion and a backbone carbonyl for the other, complete an overall distorted tetrahedral geometry for each copper ion. Given this geometric similarity, the Cu_A center can be thought of as two T1 copper centers joined together. Indeed, such a relationship has been proposed on the basis of sequence alignments and phylogenetic analyses, which indicate common ancestry for T1 copper and Cu_A proteins [45–47].

In some ways, however, the Cu_A center is quite unlike T1 copper sites. The rigid diamond core of Cu_A cultivates a special mixed valence electronic structure in the Cu(II)—Cu(I) resting state of Cu_A, such that one electron in the HOMO is fully delocalized across both copper ions, to give a [Cu(1.5)$\cdots$Cu(1.5)] oxidation state [48–54]. This electron delocalization results in some unusual spectroscopic signatures. The UV–vis absorption spectrum of Cu_A features two intense ($\varepsilon \sim 3000$–$4000\ M^{-1}\ cm^{-1}$) LMCT bands at $\sim$480 and 530 nm, due to S(Cys) $\rightarrow$ Cu CT, as well as a slightly less intense ($\varepsilon \sim 2000\ M^{-1}\ cm^{-1}$) and broad band centered at $\sim$760–800 nm [34,38,55–62]. The latter absorption arises from a Cu—Cu $\psi \rightarrow \psi^*$ transition, which occurs between the Cu—Cu bonding and antibonding orbitals [48]. The valence delocalization also produces a 7-line hyperfine splitting pattern in the EPR spectra of Cu_A centers, due to interaction of the unpaired electron with the nuclear magnetic spins of two effectively equivalent I = 3/2 copper ions [49,63,64]. Cu_A centers display even smaller $A_{||}$ values than those of T1 copper sites ($\sim$30–40 $\times$ 10^{-4} cm^{-1}) [50,55,57–59,65], reflecting even greater covalency in the copper-thiolate bonds. Calculations correlated to measurements have placed the value of this covalency at 46% Cys S-3p character in the HOMO of the ground state [50].

From the standpoint of inorganic chemistry, the dinuclear Cu_A center, with its copper–copper bond and valence delocalized resting state, is an interesting subject-matter for study. Likewise, from the perspective of biochemistry, the rare usage of Cu_A, its crucial position in such important physiological events as respiration, and its apparently redundant function (*i.e.* rapid electron transfer, like T1 copper), provoke some interesting questions about this center. Historically, devising experiments that could probe Cu_A's unique inorganic structure and answer questions about its biochemical role was not a trivial task, due to the nature of the enzymes in which Cu_A functions. In all cases, native Cu_A-containing enzymes contain other metal centers that can mask the spectroscopic signatures of Cu_A [32,35,36,38]. C*c*O, for instance, encompasses a low-spin heme *a*, that transfers electrons from Cu_A to the catalytic center, which is itself a dinuclear, heme–Cu_B site [1,22,29]. The study of C*c*O also presents the additional distinctive challenges of membrane-bound proteins, as it spans a membrane wherever it occurs. These inherent difficulties in studying native Cu_A centers spurred the development of soluble proteins, containing only the Cu_A site, by two different approaches: producing truncates of native Cu_A enzymes [38,57–62,66–69] and designing Cu_A centers into small, soluble proteins [70–73].

In one strategy used to obtain a soluble protein containing only Cu_A, the sequence of the Cu_A-subunit from C*c*O or SoxH was isolated and recombinantly expressed, sans the membrane-spanning helices that normally anchor this domain to the membrane. Such truncates have been constructed for the C*c*O from *Bacillus subtilis* [58], *Paracoccus denitrificans* [57,66,67,69], *Paracoccus versutus* [61], *Synechocystis* PCC 6803 [62], and *Thermus thermophilus* [59,60,68,69] and for SoxH from *S. acidocaldarius* [38]. The UV–vis, EPR and EXAFS spectroscopic characterizations of, as well as the reduction potentials measured for, these soluble truncates are consistent with each other [38,57,58,60–62,66–69,74–76], whereas only the truncate from *T. thermophilus* has been successfully crystallized [60]. While soluble Cu_A truncates have certainly provided important insights about Cu_A centers, the loss of interactions with other domains of their native enzymes often result in stability issues for these systems, giving them the tendency, for example, to form inclusion bodies [57].

For the other approach utilized to isolate Cu_A in a soluble protein, the minimal necessary features to form a Cu_A site were installed in a suitable protein, yielding a designed Cu_A center [70–73]. This feat was first accomplished in a copper-less quinol oxidase, where the authors recognized the same Greek-key β-barrel, cupredoxin fold in its CyoA domain that is exhibited by Cu_A domains [70]. To create the Cu_A site, they aligned the sequence of the CyoA domain with the sequences of native Cu_A domains, and searched for equivalent ligand positions in CyoA. Once they had identified corresponding locations for the ligand set of Cu_A, they introduced the Cu_A ligand set by extensive mutagenesis on the isolated cupredoxin domain. This purple CyoA remarkably bound copper in a Cu_A site, but suffered from inhomogeneity. Shortly after the release of the purple CyoA study, two other research groups independently developed designed Cu_A centers in T1 copper proteins [71,72]. Again, observing the similarity in fold of the T1 copper proteins and the native Cu_A domains, these researchers sought equivalent Cu_A ligand positions in the T1 copper proteins. However, unlike CyoA, these T1 copper proteins already contained a majority of the Cu_A ligands, as ligands to the T1 copper site. Moreover, it was recognized that a single loop between the 7th and 8th strands of the β-barrel provided most of the ligands for both T1 copper and Cu_A centers (Fig. 1A). Therefore, to introduce the Cu_A site into these T1 copper proteins, this loop was replaced with a Cu_A-forming loop. In one of the two constructs, the same loop sequence that formed purple CyoA was introduced into amicyanin, yielding Cu_AAmi [71]. This Cu_AAmi construct bound copper in a Cu_A site similar to that of native systems, as judged by UV–vis and EPR spectroscopy. For the other designed Cu_A in a T1 copper protein, the loop sequence for Cu_A from *P. denitrificans* C*c*O was introduced into azurin (Fig. 2B) [72]. The resulting Cu_AAz was easy to express in high yield and purify to homogeneity, bound copper in a Cu_A center similar to that of native systems, and, as will be discussed later in this review, became a useful platform for gaining unique insights into native Cu_A centers.

A vastly different approach taken to learn more about the Cu_A center free of other metal sites was to synthesize small-molecule mimics of Cu_A [77,78]. This proved a difficult task, because of the well-established propensity of Cu(II) to catalyze the formation of disulfide bonds between free thiols. However, varying degrees of success were met in model compounds, which duplicated some but not all of the features of Cu_A [79–96]. Tolman and coworkers have synthesized the closest small-molecule Cu_A mimic to date, which reproduces the valence delocalized dinuclear center with bridging thiolates, but has an ~0.5 Å longer Cu—Cu distance than native Cu_A centers [83]. Such small molecule mimics make important contributions to our understanding of native Cu_A centers, due to their amenability to computational techniques. Through correlation of their spectroscopic properties with computational results, a molecular orbital description of these model centers can be developed that can then be related back to biosynthetic Cu_A models and/or native Cu_A [48].

Up until the development of such model systems containing an isolated Cu_A center in the mid-1990s, many of the experiments that led to such a deep understanding of T1 copper centers, and their structure/function relationships, could not be conducted with Cu_A. Thus, many of the secrets of Cu_A's rigid diamond core and surrounding protein environment, and their bearing on the function of this center, had yet to be unlocked. In Section 3, we discuss the contributions made by the biosynthetic Cu_AAz model to revealing these secrets.

1.2. The biosynthetic approach to the study of metalloenzymes

Metalloenzymes catalyze numerous important processes in biological systems, from the challenging chemistry of oxygen reduction [32], water oxidation [97], and methane oxidation [98], to deceptively simple electron transfer reactions (including those catalyzed by T1 copper and Cu_A centers) [5]. It has recently been estimated that over half of the entire proteome consists of metalloproteins [99]. To duplicate these amazing functions, for example, in alternative energy applications, as well as to treat diseases caused by their malfunction, it is desirable to both understand these metalloproteins and to construct similar catalytic centers. In order to study metalloprotein functions, there are two strategies that can be applied (Fig. 2): a "top-down" approach, in which the native metalloproteins are subjected to mutagenesis, and the perturbation to their structure and/or function are measured (Fig. 2A), and a "bottom-up" approach, in which a model containing the basic components of the native metal centers is built (Fig. 2B). While these two approaches are complementary, the "bottom-up" approach has several advantages over the traditional "top-down" approach. One advantage is that the minimum features needed for function can be identified. Another advantage is that the systems designed by the "bottom-up" approach are often simpler than the native systems, allowing deconvolution of their properties from other factors in the native environment, such as other metal centers.

Traditionally, the only realistic option for using the "bottom-up" approach to model metalloenzyme centers was to synthesize small molecule analogs of these sites. While there have been some great successes using this approach [78], small molecules can only mimic the protein environment to a certain extent. In particular, the secondary coordination sphere of metal centers in proteins

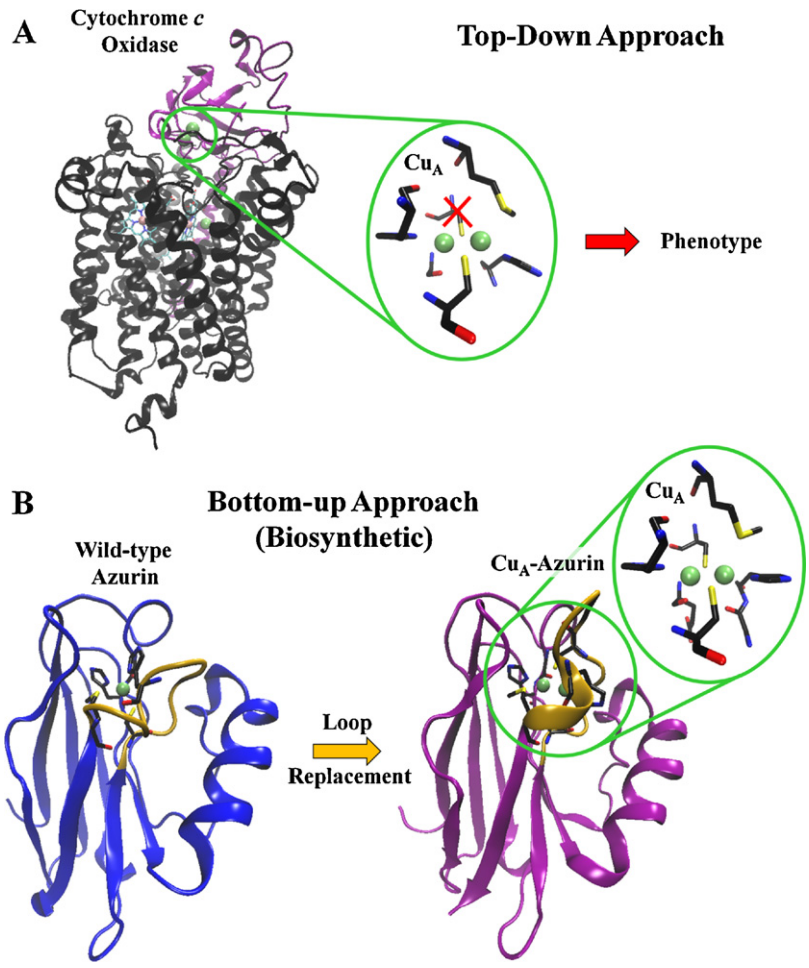

Fig. 2. Contrasting examples between the complementary top-down (A) and bottom-up (B) approaches to studying metal centers in biological systems. In the top-down approach (A), a native metal center is perturbed, usually by site-directed mutagenesis, such as mutation of one bridging Cys in Cu_A of CcO, and the resulting changes to the system are measured. Measurements of the perturbation to the Cu_A of CcO must be performed on the membrane-bound enzyme complex, in the presence of the other metallocofactors (two hemes and a copper site). In the biosynthetic take on the bottom-up approach (B), a minimal model of the metal center is constructed in a protein free of other metallocofactors. In this example, the ligand loop of the T1 copper protein azurin was replaced with the corresponding ligand loop of a Cu_A center from a native CcO, and the resulting Cu_A–azurin biosynthetic model bound copper in a site very similar to those of native Cu_A enzymes [72]. The minimal model here, then, is built from one His ligand of the original T1 copper center and the ligand loop from a native Cu_A, as the sequence identity between the other portions of azurin and the native Cu_A subunit are low. PDB IDs: (A) 1XME, (B) 4AZU (wild type Az), and 1CC3 (Cu_AAz).

has been demonstrated in a number of cases to be very important for their functions [4,8,9,100–135]. Synthesizing large enough ligand scaffolds to incorporate these secondary coordination sphere interactions, let alone controlling them, is difficult at best. Nevertheless, synthetic chemists have undertaken the incorporation of these secondary coordination sphere effects [136–138], and in so doing, highlighted how important they are.

With the advent of modern molecular biology techniques, the option of creating "bottom-up" models (Fig. 2B) of metalloproteins in protein scaffolds became more feasible. This method of modeling native metal centers has recently been thoroughly reviewed [139–142], and will only be briefly summarized here. In this approach, the protein can be simplistically regarded as a very large ligand to the metal, and thus, instead of a synthetic model, the resulting construct is a biosynthetic model. Practically speaking, however, the biosynthetic "ligand" for the target metal center must be carefully chosen to reflect the requirements of this center. Ideally, one would be able to choose a sequence of amino acids that would fold and chelate the metal in the desired fashion. This take on biosynthetic modeling is called "*de novo* design," from the literal Latin translation of "from the beginning" [99,143–148]. While it represents the ideal for generating a biosynthetic model, and a number of groups have made great progress in this field [99,143–149], our current understanding of how polypeptides fold into three-dimensions from a primary sequence of amino acids limits the implementation of this method.

Instead, we can take advantage of Nature's selection of well-folded, stable proteins, as well as the ever increasing volume of 3D structures available for proteins, and set certain criteria for a biosynthetic ligand [142]. These criteria can range from very basic, like an unoccupied space for the metal to fill, to quite complex, like subtle orientations of potential amino acid ligands, to optimize overlap with the metal's valence orbitals [141,142]. Computational methods can greatly simplify the process of choosing a biosynthetic ligand, but have generally lacked the required sophistication, particularly in handling transition metals and their preferred ligand geometries [150]. Once a protein scaffold has been chosen, molecular dynamics (MD) of the conceptualized design, with its various amino acid mutations, can provide some indication of how successful the design will be [151,152]. However, MD computational results must be interpreted cautiously, as this type of energy minimization only considers electrostatic and steric effects. Thus, a drawback of using the biosynthetic approach to metalloprotein modeling is that designing the model systems is often quite challenging. On the flipside, once you have a successful design, incorporating subtler features, such as hydrogen bonding to metal

ligands, is much more feasible than in small molecules. Moreover, the model attained through the biosynthetic approach, as opposed to the synthetic approach, is closer to native metalloenzymes in several other ways, such as the immediate dielectric around the metal ion, the water solubility of the overall complex, and the types of functional groups available to interact with the metal ion.

A third method for metalloenzyme modeling is a semi-biosynthetic one, in which the majority of the ligand is a recombinantly expressed polypeptide, while a small section of polypeptide is synthesized separately [139,153]. This approach enables the incorporation of unnatural amino acids, which supply metal ligands other than the handful offered by amino acid side chains. Section 2 elaborates upon this approach in greater detail.

A number of native metal centers have been successfully modeled by the biosynthetic approach [139–142], including those discussed in this review. These successful biosynthetic models have provided insights that would be difficult or impossible to obtain from the native equivalent. For example, biosynthetic models are typically purified in the metal-free form, allowing substitution of other metal ions to probe the importance of the metal identity and/or charge, whereas this is often not possible in native metalloproteins. As the computational methods for designing biosynthetic models of metalloenzymes improve, we look forward to the development of a greater number of biosynthetic models from which to gain deeper understanding of native metal centers.

2. Probing properties of the type 1 copper site in azurin using a semi-biosynthetic approach

To elucidate its unique spectroscopic properties, as well as its electron transfer properties, various spectroscopic methods and theoretical calculations have been applied to azurin and other blue copper proteins [8,15]. In addition to studies of the wild type proteins, mutagenesis has been used to probe the role of important residues, including the copper ligands. In azurin, Met121 has been mutated to all of the other 19 amino acids, and His46 and His117 have been mutated to Gly, all of which left the intense LMCT band and blue color of azurin intact [154–156]. As the Cu—S(Cys) bond defines the properties of type 1 copper sites [8], mutation of Cys to other amino acids will dramatically alter the copper site. Substitution of any other amino acid for Cys will result in loss of the intense LMCT charge transfer bands, arising from the interaction of the Cys-S with copper. Mutation of Cys to Asp makes azurin a type 2 copper protein, as demonstrated by large hyperfine splittings ($A_{||} \sim 152 \times 10^{-4}\,cm^{-1}$) in the EPR spectrum and a slow electron transfer rate [157–160]. Addition of another mutation, to make Cys112Asp/Met121Glu Az, results in a novel copper site, called type zero copper, which has the small parallel hyperfine splittings and rapid electron transfer rates characteristic of T1 copper centers, but no longer fits the classification of T1 copper due to the loss of the copper-thiolate interaction [161–164].

The use of mutagenesis to probe the properties of T1 copper centers has revealed important features of these centers. However, due to the limited number of natural amino acids, especially those capable of coordinating a metal ion, it is impossible to fine-tune the ligand set of T1 copper centers. The appealing option to accomplish such fine-tuning of the ligand set is to incorporate non-native amino acids, having the desired ligand side-chains, into the T1 copper center. Developments in the fields of biochemistry and chemistry have provided several options for the incorporation of unnatural amino acids into proteins, including total synthesis of the protein [165], ligation of two peptides [166,167], cavity

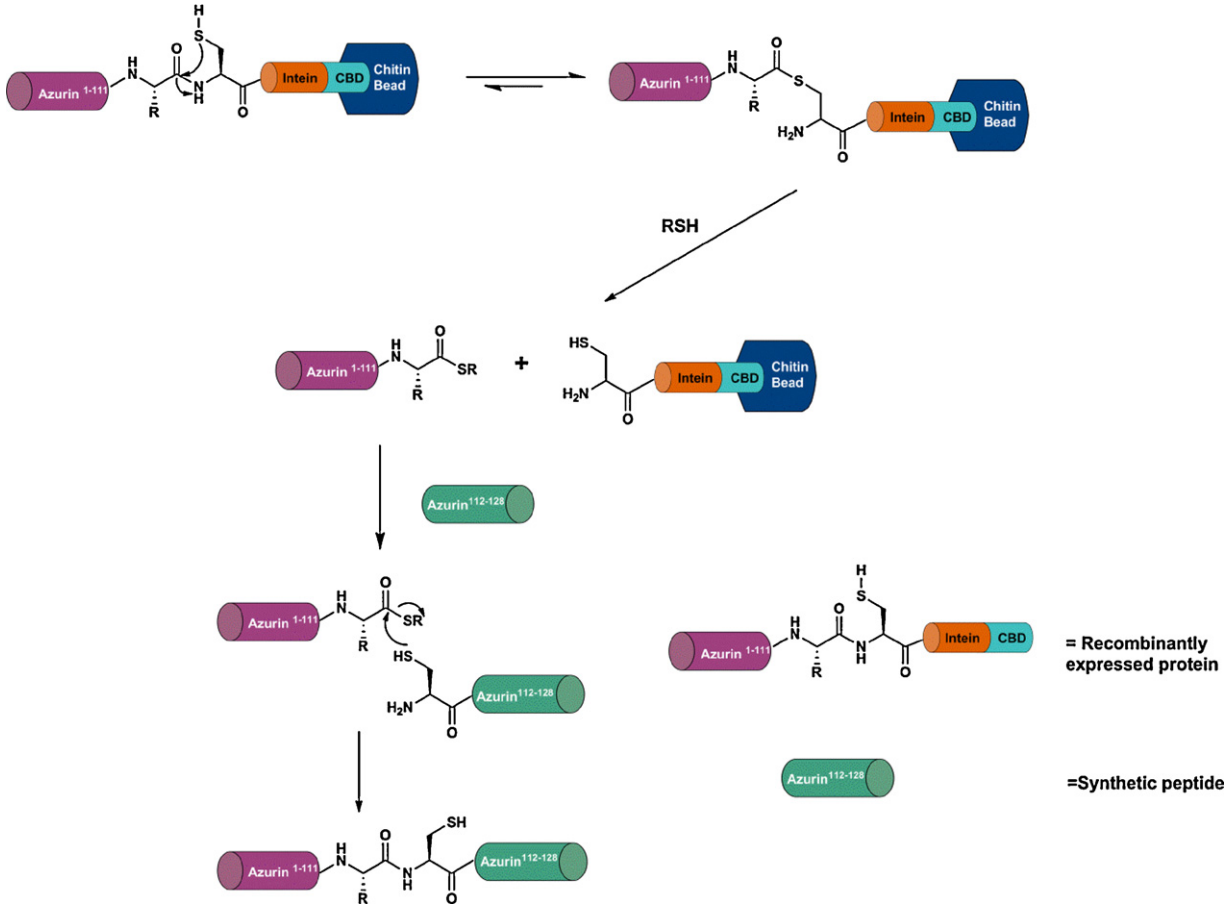

Fig. 3. Scheme of EPL using azurin as an example.

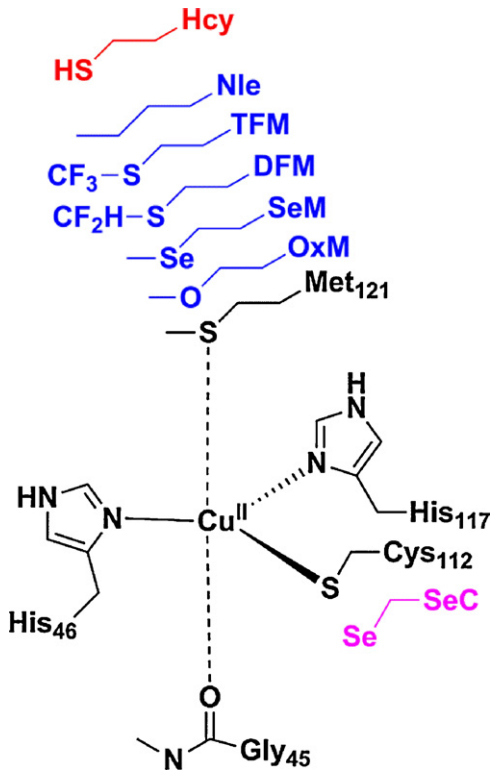

Fig. 4. T1 copper site in azurin and unnatural amino acids used to replace copper ligands [172,173,175,176].

complementation [155] and engineered tRNA/tRNA synthetases for *in vivo* incorporation [168,169].

One such technique for incorporating unnatural amino acids, called expressed protein ligation (EPL), was developed based on native chemical ligation and the chemistry of intein, which is a segment of a protein that is able to excise itself and rejoin the remaining portions with a native peptide bond [167,170,171]. As shown in Fig. 3, a peptide fragment of the target protein is fused with intein, which is a self-splicing protein domain, and this fusion is recombinantly expressed. After purification, external thiol is added to trigger intein cleavage, producing a thioester peptide. In accordance with the process of native chemical ligation, the thioester peptide will react with a chemically synthesized peptide with an N-terminal Cys to yield the full length protein of interest [167,170,171].

Azurin is an ideal protein for EPL. It has a cysteine close to its C-terminus, and 3 of the 5 ligands are in last 17 amino acids (Cys112, His117 and Met121), making them accessible to EPL. The author's group has used this method to study the electronic structure, spectroscopic properties and reduction potential of azurin through the incorporation of various unnatural amino acids, particularly at the Met121 and Cys112 positions (Fig. 4) [172–175].

2.1. Contributions of Cys and Met sulfurs to electronic structure unveiled by unnatural amino acids

Various spectroscopic methods and theoretical calculations have shown that a highly covalent S—Cu bond dominates azurin's spectroscopic properties (see Section 1.1.1). Despite intensive study on the native protein and its mutants, some questions about the protein remained unanswered. For example, while S K-edge XAS indicated a high degree of Cu—S covalency, it is impossible to differentiate by this technique the contribution of S from Met versus S from Cys [8]. Se is in the same group as S, and thus possesses the same valence shell structure. Selenocysteine (SeC) and selenomethionine (SeM) are electronically similar to Cys and Met and sterically equivalent to these canonical amino acids. Therefore, it was postulated that replacing Cys and Met by SeC and SeM would cause minimal perturbation and provide good probes for these two amino acids. Using the aforementioned EPL method, both SeC and SeM were incorporated into azurin, generating Cys112SeC and Met121SeM variants [172,173]. The UV–vis and EPR spectra of Met121SeM azurin were essentially identical to WT azurin [173]. On the other hand, Cys112SeC displayed a red-shifted LMCT band at 677 nm and a significantly increased parallel hyperfine splitting value ($A_{||} = 99 \times 10^{-4}\,cm^{-1}$) compared with WT azurin ($A_{||} = 67 \times 10^{-4}\,cm^{-1}$), while still maintaining the essential characteristics of T1 copper centers [172]. Solomon and coworkers have used a suite of spectroscopic methods, including S K-edge XAS, MCD, and resonance Raman, together with DFT calculations to study the proteins [177]. The pre-edge of Met121SeM azurin exhibited similar S character in the $S_{thiolate}$ 1s-$\psi^*_{\beta\text{-LUMO}}$ bond (within 3% error) as in WT, indicating that S_{Met} does not contribute significantly to S—Cu covalency. Due to the lower electronegativity of Se as compared to S, there is a smaller HOMO–LUMO gap, leading to a red shift of the corresponding S(Cys)/Se(SeC)$_{p\pi}$—Cu charge transfer band in the UV–vis and MCD spectra. Despite the slight lengthening of the S_{Cys}/Se_{SeC}—Cu distance (from 2.16 Å to 2.30 Å) [174], resonance Raman demonstrated that there was little change in the force constant of this bond in Cys112SeC azurin, indicating that the bond strength was not diminished in Cys112SeC Az [177].

2.2. Unnatural amino acids reveal a reduction potential tuning strategy

While many T1 copper proteins contain an axial methionine, this residue is not strictly conserved. Mutagenesis to all other 19 amino acids has been performed and results in no significant changes in the spectral features [154,178–180]. Based on calculations and spectroscopic and mutagenesis studies, various different roles have been proposed for the axial methionine, including protecting the copper site from exogenous ligands [179,181–185], controlling the geometry of the copper center [186–191], modulating the S_{Cys}—Cu interaction [154,186,192,193] and tuning the reduction potential [13,194]. Due to the limited selection of natural amino acids, it is difficult to alter only one factor while keeping others unchanged using standard mutagenesis. To pinpoint the function of methionine in reduction potential tuning, a series of isostructural unnatural amino acids were introduced to the Met121 position [174,175]. These mutants exhibited little change in their UV–vis and EPR spectra, while spanning a ~300 mV range of reduction potentials. The observed variation in reduction potential correlated linearly with the hydrophobicity of the axial ligand [174,175], revealing the mechanism by which the axial methionine tunes the reduction potential of T1 copper proteins. Once this principle of axial Met tuning was ascertained, it was subsequently used in combination with changes to the secondary coordination sphere to achieve a series of azurin mutants extending over a 600 mV range of reduction potentials, with gradual variation of approximately 50 mV between the individual mutants [132]. Thus, the principle revealed through the incorporation of unnatural amino acids may play a large part in the development of designer T1 copper proteins, for use as water soluble, green redox reagents.

2.3. The coupled distortion model elegantly illustrated in a single protein using an unnatural amino acid

Besides typical T1 copper proteins like azurin and plastocyanin, there are also naturally occurring "perturbed" T1 copper proteins, as in, for example, cucumber basic protein and nitrite reductase.

These proteins have an additional ~400 nm absorption peak in their UV–vis spectra, as well as rhombic EPR signals. At the same time, the "perturbed" T1 copper proteins have longer Cu—S(Cys) distances and shorter Cu-axial ligand distances [13]. A newly discovered protein, nitrosocyanin, displays the greatest perturbation, with dominant ~400 nm absorption in its UV–vis spectrum and large hyperfine splittings ($A_{||} \sim 150 \times 10^{-4}\,cm^{-1}$) in its EPR spectrum, to the extreme that it is no longer considered a T1 copper center, but rather, a T2 copper site [195,196]. According to its crystal structure, nitrosocyanin has an additional equatorial water ligand and a Glu as an axial ligand, instead of Met [195].

Due to the differences in their electronic absorptions, those proteins show different colors, from blue (T1 copper) to green ("perturbed" T1 copper) to red (T2 copper in nitrosocyanin). The electronic structures of these proteins and the origin of the transition between their properties have been elucidated by Solomon and coworkers through a suite of spectroscopic methods in combination with theoretical calculations [13,15,197]. In the resulting "coupled distortion" theory, Solomon and coworkers state that shorter Cu-axial ligand distances result in distortion of the T1 copper geometry toward tetragonal, which elongates the Cu—S(Cys) distance [13]. This distortion renders the $p_{\sigma(Cys)}$-Cu CT more favorable than $p_{\pi(Cys)}$-Cu CT, which is manifested as an increase in the ~400 nm absorption over the ~600 nm absorption in the UV–vis spectrum.

The transition from blue to green copper has been accomplished in the same scaffold by manipulating the axial ligand strength of T1 copper proteins. By changing a weak Met to His [179,190,198] or Glu [199–201], the blue copper protein azurin can be converted to a green copper protein. By mutating Met to a weaker Thr, the natively green copper protein, nitrite reductase, has been converted to blue copper protein [202].

Despite these achievements using standard mutagenesis, conversion between blue and red copper proteins has not been realized before. By mutating the axial Met to the stronger ligands, cysteine and homocysteine (Hcy), the latter able to close the distance to the Cu ion, the blue copper protein azurin was converted to a green and a red copper protein, respectively (Fig. 5) [176]. Met121Cys azurin has an ~450 nm absorption in addition to the 625 nm peak present in WT azurin. In Met121Hcy azurin, the ~410 nm band dominates over the 625 nm peak, bestowing the protein with a red color. EPR of Met121Hcy azurin displays a large hyperfine splitting ($A_{||} \sim 180 \times 10^{-4}\,cm^{-1}$), similar to nitrosocyanin. Additionally, EXAFS analysis has shown that the axial ligand to Cu distance decreased from WT azurin (>3 Å) to Met121Hcy azurin (2.79 Å). Thus, incorporation of Hcy into azurin through the use of EPL led to an illustration of the coupled distortion theory in a single protein.

3. A unique window into the workings of Cu_A centers by way of a biosynthetic Cu_A in azurin

As discussed in Section 1.1.2, native Cu_A centers are challenging to study, due to the presence of other metal centers in the same enzymatic complexes, which are often embedded in a membrane. Fueled by this problem, a model Cu_A in azurin was constructed using the biosynthetic approach. In this section, we discuss some of the advances realized in our understanding of Cu_A centers through the study of this biosynthetic Cu_AAz model.

3.1. Cu_AAz closely reproduces spectroscopic and geometric features of native Cu_A centers

For any model of a native metal center to be considered valid, it should at minimum reproduce the major characteristics of the site after which it is modeled. A list of such features for Cu_A models should include most or all of the following: (1) a dinuclear copper site, (2) bridging thiolates between the copper ions, (3) a mixed-valence, valence-delocalized resting state, (4) a copper–copper bond, and (5) equatorial His imidazolyl ligands or equivalent. Evaluation of how well a model meets these criteria requires a combination of spectroscopic and structural information.

Early studies of the Cu_AAz biosynthetic model established that its spectroscopic characteristics were similar to native Cu_A centers and that it bound two copper ions (Fig. 6) [48,72,203–206]. The UV–vis absorption spectrum of Cu_AAz features two S(Cys) → Cu CT bands at 485 ($\varepsilon \sim 3700\,M^{-1}\,cm^{-1}$) and 530 nm ($\varepsilon \sim 3400\,M^{-1}\,cm^{-1}$) [48,204], compared to 480–485 and 530–540 nm for native Cu_A centers [7]. Cu_A in azurin also featured a broad band centered at 760–800 nm ($\varepsilon \sim 2000\,M^{-1}\,cm^{-1}$), typical of the Cu—Cu $\psi \rightarrow \psi^*$ transition, suggesting that Cu_AAz had reproduced the copper–copper bond [48,204]. Additionally, the EPR spectrum of Cu_AAz displayed a 7-line hyperfine splitting pattern, demonstrating that this biosynthetic model duplicated the mixed-valence, valence delocalized ground state of native Cu_A centers [204]. EXAFS, CD, MCD, and resonance Raman analyses of the Cu_A in azurin also suggested a high level of electronic and structural identity with Cu_A centers from CcO [48,72,203–205]. Perhaps

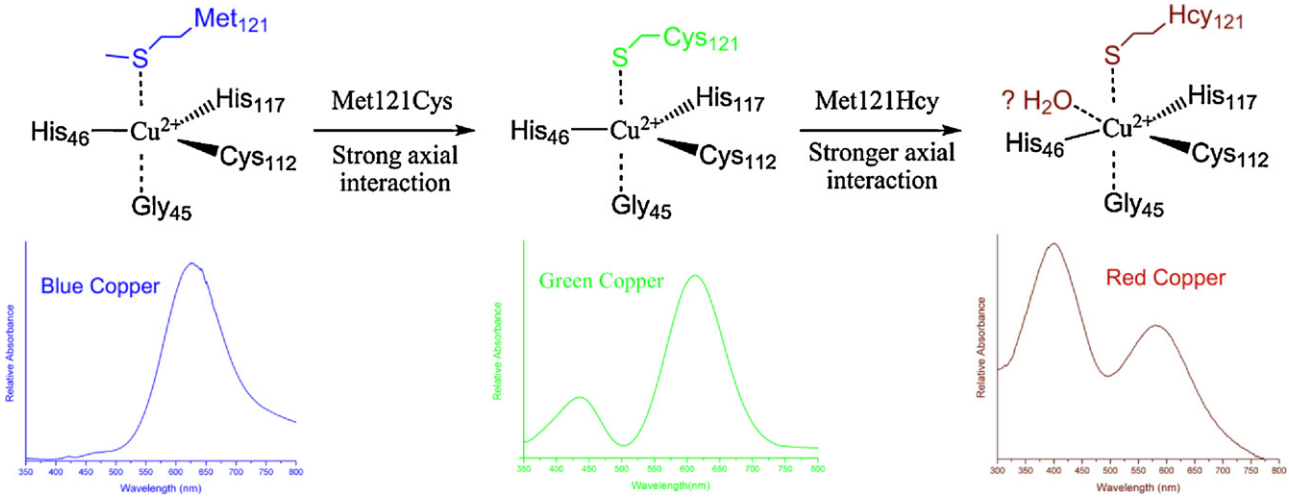

Fig. 5. Conversion of blue copper protein azurin to green and red copper protein by changing axial Met to Cys and Hcy.
Reprinted with permission from [176]. Copyright 2010 American Chemical Society.

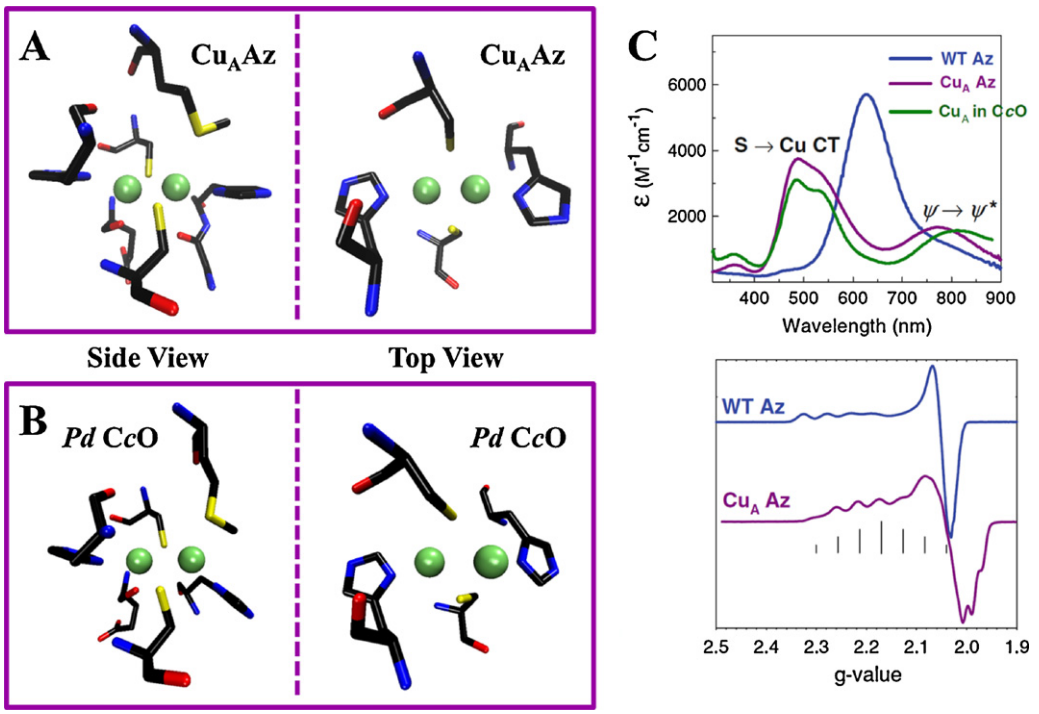

Fig. 6. Comparison of Cu_A centers in (A) the biosynthetic Cu_AAz model (PDB ID 1CC3) and (B) native *Paracoccus denitrificans* (*Pd*) CcO (PDB ID 3HB3), from both a side view (left) and a top view (right). The basic structural features of the Cu_A center are exhibited in Cu_AAz. (C) UV–vis absorption (top) and EPR spectra of Cu_AAz, WT Az and a CcO. Adapted from Ref. [28] with permission from Society of Biological Inorganic Chemistry.

the greatest confirmation of Cu_AAz as a valid structural model of native Cu_A centers came with its X-ray crystal structure [207]. Comparison of the Cu_A observed in the Cu_AAz structure with that of a Cu_A from CcO showed a very similar arrangement of ligands about the copper ions, and a copper-copper distance that was even slightly shorter than that in CcO, confirming the presence of a Cu—Cu bond. Thus, a variety of spectroscopic techniques and X-ray crystallography all demonstrate that Cu_AAz is a good electronic and structural model of native Cu_A centers.

3.2. Assembly of the Cu_A center illuminated via copper addition to the metal-free site

One aspect of native Cu_A centers which is still not fully understood is how these sites become metalated *in vivo*. In the cytoplasm, copper levels are rigorously regulated, such that the free copper levels in cells are extremely low, estimated to be in the attomolar range [208–214]. Thus, in order to acquire their cofactor, copper proteins localized within the cell must receive copper ions from other proteins, called metallochaperones. Such a chaperone, named Sco, has been proposed for Cu_A from CcO. However, metalation of Cu_A by this protein has yet to be demonstrated, and its role as a metallochaperone has been called into question [215]. Whereas CcOs from eukaryotes are localized within the mitochondria [1], in CcOs from Gram-negative bacteria, Cu_A is exposed to the periplasmic space, while for Gram-positive bacteria, Cu_A in CcO extends into the extracellular space [29,211,216,217]. N_2OR also exists as a soluble protein in the periplasmic space [218]. In these scenarios, copper levels are regulated less tightly or not at all compared to inside the cell, suggesting that metalation of Cu_A in these instances may be unmediated by metallochaperones [211]. In fact, this scenario of unmediated Cu_A metalation has been considered as a possibility for Cu_A in N_2OR [35,219,220]. Another unknown in the metalation of Cu_A centers is the oxidation state of the copper ions that are inserted. The final resting state of Cu_A consists of a Cu(II) and a Cu(I) ion. All confirmed copper chaperones carry copper as Cu(I) [209–214]. However, the Cu(II) state of Sco is highly stable [221], and has proven essential for the function of this protein [215,222,223]. Moreover, the redox environment of the periplasm permits the existence of both Cu(I) and Cu(II), while Cu(II) is the stable oxidation state in the extracellular space [211]. Thus, currently, the mechanism of Cu_A metalation *in vivo* is poorly understood.

Although studies of *in vitro* metalation of Cu_A centers may not perfectly reflect the conditions of *in vivo* Cu_A metalation, such studies could provide important insights into this process. Moreover, as discussed above, prokaryotic Cu_A enzymes may acquire copper through a relatively unregulated pathway. Therefore, *in vitro* studies of Cu_A metalation may closely reflect the metalation mechanisms of prokaryotic Cu_A enzymes. Summarized here are three such *in vitro* studies of Cu_A metalation, two in Cu_AAz and one in N_2OR.

In an early study of Cu_AAz, the metalation of the apo-protein was followed by stopped-flow UV–vis spectroscopy upon addition of a ten-fold excess of $CuSO_4$ at pH 5.1 [224]. In this experiment, a single intermediate was observed, with intense absorption at ~385 nm. Intense absorption in the region of 360-400 nm is characteristic of the Cys-S → Cu CT bands of type 2 (T2) copper centers, which adopt tetragonal geometries [7,15]. This T2 copper intermediate formed rapidly, with $k_{obs} = 1.2 \times 10^3\ s^{-1}$. The ~385 nm band of the T2 copper intermediate subsequently decayed, with $k_{obs} = 3.1\ s^{-1}$, while the absorptions due to Cu_A concomitantly increased. This second process was accompanied by an isosbestic point between the ~385 nm band and the ~485 nm band of Cu_A, indicating conversion of the T2 copper intermediate to Cu_A. As only Cu(II) was supplied for this reaction, reducing equivalents must be supplied by the system. Addition of ascorbate or Cu(I) increased the yield of Cu_A centers, suggesting that the active site thiols of the Cu_A center itself were providing the reducing equivalents. Indeed, the Cu(II)-catalyzed oxidation of free thiols to disulfide is widely known to be quite facile [225–227], and in this case, is additionally an intramolecular reaction. From these observations, a mechanism was formulated (Fig. 7A) in which the metal-free protein reacts with Cu(II) to form

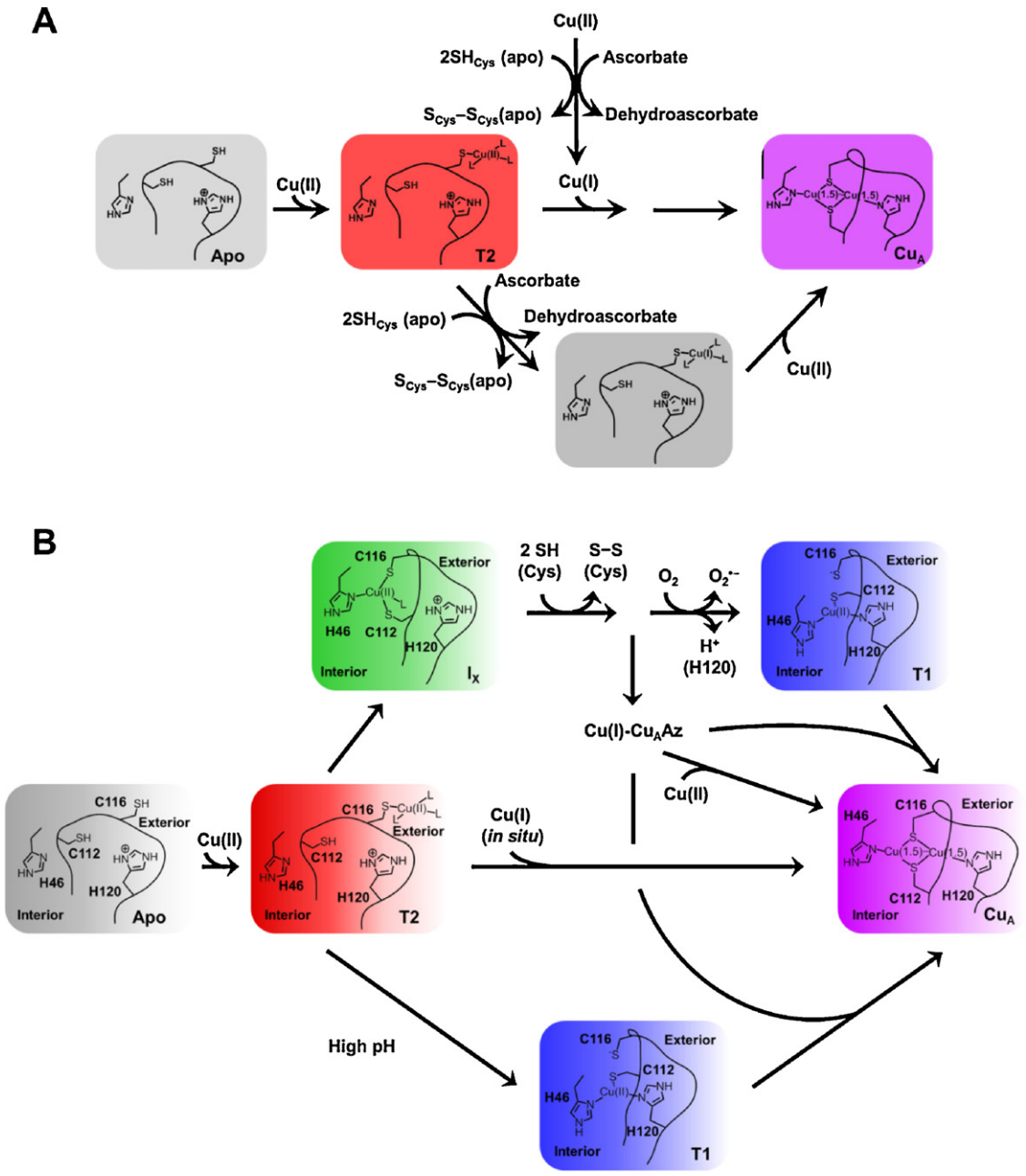

Fig. 7. (A) Mechanism of copper incorporation into the Cu_A site of Cu_AAz formulated from ten-fold excess $CuSO_4$, stopped-flow UV–vis studies [224]. (B) Mechanism of copper incorporation into the Cu_A center of Cu_AAz formulated from sub-equivalent $CuSO_4$, stopped-flow UV–vis and EPR spectroscopic, as well as mutagenesis, studies [228]. The label "Cu(I) (*in situ*)" refers to Cu(I) that has been generated upon the addition of Cu(II) alone, through reduction by the active site cysteines of Cu_AAz, or by an exogenously added reductant, such as ascorbate. The labels "interior" and "exterior" refer to the interior and exterior of the protein, respectively.
Reprinted with permission from [228]. Copyright 2011 American Chemical Society.

a capture complex with one of the active site Cys residues, *i.e.* the T2 copper intermediate. This intermediate is then either itself reduced to Cu(I) by active site thiols, followed by incorporation of a Cu(II) ion, and/or reacts with Cu(I) generated elsewhere through reduction of Cu(II) by active site thiols, to form the final mixed-valence Cu_A center.

More recently, a similar study was undertaken in N_2OR from *P. denitrificans* [28]. During the Cu(II) metalation of this Cu_A center, two intermediates were observed to form on similar timescales, one with spectral features typical of T2 copper centers with thiolate ligation, and another with the characteristics of a T1 copper center. Again over similar timescales, both of these intermediates decayed, as indicated by loss of their UV–vis absorptions, with simultaneous increase of the absorptions due to Cu_A. Isosbestic points were present between the major absorption bands of both intermediates and the neighboring Cu_A absorption bands, strongly suggesting conversion of these intermediates to Cu_A. Although these isosbestic points provide clues, the mechanism of Cu_A formation from these intermediates has yet to be ascertained. Again, inclusion of Cu(I) during the copper incorporation increased the yield of Cu_A centers, supporting the generation of Cu(I) in the system from oxidation of the active site cysteines. The formation of both of these types of mononuclear copper centers from the ligand set of a native Cu_A provided experimental support for a

previously proposed evolutionary link between these types of copper centers [45–47]. Additionally, a pH-dependence for the copper incorporation process was observed, such that at low pH, the intermediates accumulated to a lesser extent, and Cu_A formed more rapidly, while the opposite was true at high pH. Since lower pH apparently facilitated more rapid assembly of the Cu_A centers, it was proposed that the low pH environment of Cc*O*s and SoxH aided in correct assembly of their Cu_A cofactors.

In light of the observation of both T1 copper and T2 copper intermediates in the Cu_A ligand set of N_2OR, the Cu(II)-dependent metalation of Cu_AAz was revisited, to see if a similar T1 copper intermediate formed under conditions other than those investigated previously. Moreover, while the ten-fold excess copper condition used previously simplified the kinetics to pseudo-first order, such a condition does not likely mimic the typical copper concentrations experienced by Cu_A centers *in vivo*. Therefore, kinetic studies of the Cu(II)-driven metalation of Cu_A in Cu_AAz were undertaken, varying both copper concentration and pH [228]. When the Cu_AAz concentration was greater than the $CuSO_4$ concentration, both T2 copper and T1 copper intermediates were observed, similarly to N_2OR. Global fitting of the UV–vis absorption kinetic data permitted interpretation of a complex copper incorporation mechanism (Fig. 7B), involving yet a third intermediate, intermediate X (I_X). Time-dependent EPR provided further evidence for the intermediates, and spin-counting of these EPR spectra informed on when Cu(I) was being generated in the system. Oxygen-dependent UV–vis stopped-flow revealed a positive correlation between the amount of dissolved oxygen and formation of the T1 copper center.

Additional information about the intermediates came from comparisons to previously studied active site mutants of Cu_AAz [229]. When Cys112 was mutated to Ser, a T2 copper site formed, with similar UV–vis and EPR spectra to the T2 copper intermediate. It can be inferred then that the T2 copper intermediate is a capture complex with Cys116, which is also supported by the greater solution accessibility of this residue, compared to Cys112. Conversely, when Cys116 was changed to Ser, a T1 copper center formed, with nearly identical UV–vis and EPR spectra to the T1 copper intermediate. Therefore, the assignment of the T1 copper intermediate arising from a complex with Cys112 could be made with great confidence. In the case of I_X, the assignment of this intermediate was made difficult by the fact that the spectroscopic properties did not readily suggest a known natural copper center. The closest analog of I_X, as judged by spectroscopic parameters, was a Cu(II)-dithiolate complex formed in Cu(II)-substituted liver alcohol dehydrogenase [230–233]. Therefore, it was proposed that I_X was a Cu(II)-dithiolate, involving both active site cysteine residues, which was also consistent with other aspects of this intermediate (see below).

Altogether, these experiments enabled the formulation of a unified copper incorporation scheme for Cu_A in Cu_AAz upon addition of Cu(II) (Fig. 7B). First, a T2 copper capture complex is formed with Cys116, from which two pathways are operational. The first pathway results in direct Cu_A formation, and was observed previously under ten-fold excess $CuSO_4$ conditions. In the kinetic model, this step was fit by a bimolecular rate equation, which could account for the copper dependence. Through the second pathway, the T2 copper intermediate converts to I_X, which is proposed to accompany a conformational change in the protein, as this first-order step is quite slow, ~0.2–0.9 s^{-1}. A conformational rearrangement during this step is also consistent with a need to rotate the capture complex with Cys116 into the Cu_A binding site, to provide access to Cys112, as we propose that I_X is a Cu(II)-dithiolate. Spin-counting of the time-dependent EPR spectra revealed that the next step, loss of I_X, is attended by a decrease in overall spin in the system. This loss of spin in turn suggests that the product of I_X decay is Cu(I). This behavior of I_X is also in line with its assignment as a Cu(II)-dithiolate complex, as such complexes are prone to autoreduction of the copper ion and oxidation of the thiols to disulfide [225–227,232,233]. The oxygen-dependence data then point to oxidation of a Cu(I) product of I_X decay to the T1 copper intermediate. This T1 copper intermediate shares an isosbestic point with the absorptions from the subsequently formed Cu_A center, supporting the kinetic model for this step of T1 copper converting to Cu_A. Formation of Cu_A in this step is presumably accomplished by reaction of the T1 copper intermediate with Cu(I), to make the mixed-valence Cu_A center.

The observation of both T2 copper and T1 copper centers in the ligand set of Cu_A from Cu_AAz provides confirmation that the relationship between these three types of sites is universal to all Cu_A centers. This kinetic study of Cu(II) incorporation into Cu_AAz also reiterated that Cu_A centers can assemble from unregulated copper in its environmentally stable oxidation state. However, the total number of successfully assembled Cu_A centers was only ~30% of the sites in all protein molecules. The use of the active site Cys residues as sacrificial reductants leads to significant waste. Thus, while some native Cu_A centers are in positions where this metalation scheme could apply (see above), it is unlikely that this seemingly straightforward approach to Cu_A assembly occurs *in vivo*. Nevertheless, nature has developed a means of correcting the oxidation state of a thiol/disulfide couple by use of the thioredoxin class of proteins [234,235], rendering this method of Cu_A metalation only an unlikely possibility, not an unfeasible one.

3.3. Axial Met influences reduction potential to a lesser extent than in the corresponding type 1 copper site

As discussed in Section 2.2, the reduction potential of T1 copper centers is tuned across ~300 mV by changes to the hydrophobicity of the axial Met position. Since a similar axial Met ligand is conserved across all Cu_A centers, the question of whether or not this axial position could tune the reduction potential of Cu_A in a similar manner arose. To answer this question, the axial Met in Cu_AAz was mutated to Asp, Glu, and Leu, which together cover the extremes of the hydrophobicity series among the natural amino acids [236]. The reduction potentials measured for these axial Met variants showed very little change from original Cu_AAz, spanning only ~20 mV (Fig. 8), despite some visible perturbation to the UV–vis and EPR spectra of these mutants. The significantly smaller axial tuning effect in Cu_AAz may reflect the resilience of the diamond core of Cu_A. The stability of the interactions making up the diamond core—the bridging Cys thiolates and copper–copper bond—may lead to greater resistance to perturbations arising from the axial position.

However, a recent study in the soluble Cu_A truncated domain from *T. thermophilus* (*Tt*) [76] suggests that, if it is the diamond core that enables Cu_A in azurin to withstand perturbations from the axial position, there is a limit to how far the Cu_A diamond core can resist such changes. In this study, a different set of axial Met mutants was generated, with Met replaced by Gln, His, Ser, Tyr, and Leu. Unlike in Cu_AAz, the resulting changes to the reduction potential were similarly large as those seen in T1 copper proteins, spanning ~200 mV. The difference in behavior between the *Tt* Cu_A and Cu_A from azurin was attributed to the difference in Cu—Met bond length in these two systems: 2.47 Å and ~3.07 Å (avg. of two molecules in the asymmetric unit), respectively (Fig. 9). Another hypothesis for this difference in behavior between *Tt* Cu_A and Cu_AAz, which falls in line with the argument that the diamond core enforces the similar reduction potentials, is that the diamond core in Cu_AAz is actually stronger than that in most Cu_A centers, as it contains the shortest Cu—Cu bond at ~2.4 Å (Fig. 9).

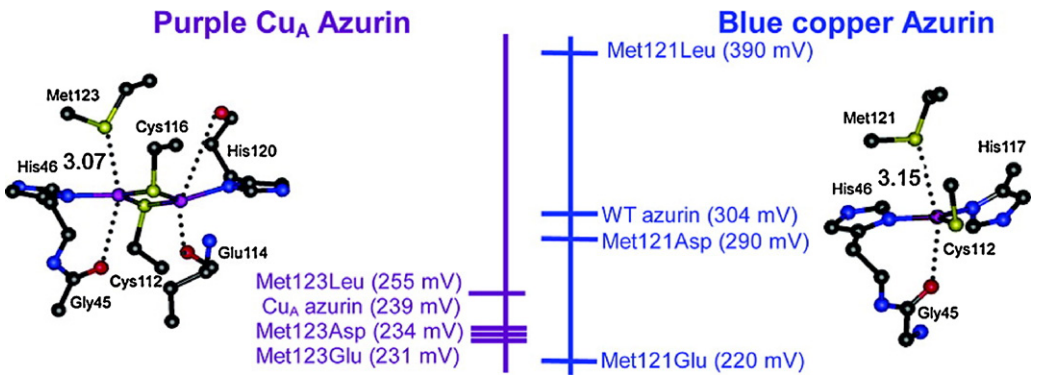

Fig. 8. Comparison of reduction potential tuning demonstrated by the axial Met position in Cu_AAz (left) versus WT Az (right), which shows that the effects of changes to this position on the reduction potential in Cu_AAz are dramatically smaller than those in WT Az.
Reprinted with permission from [236]. Copyright 2005 American Chemical Society.

3.4. Mutations to His and Cys ligands: the curiously stable diamond core of Cu_A

Cu_AAz's small size and relative ease of expression and purification make this biosynthetic model highly amenable to mutagenesis studies. As covered already in the previous section, mutations to the axial Met position appear to perturb the site minimally, at least in terms of function. One might expect, though, that mutation of an equatorial His ligand, at a bonding distance of just over 2 Å, would result in significant perturbation of the Cu_A site, even loss of copper binding. However, mutation of His120 to Ala yielded a UV–vis spectrum strikingly similar to that of original Cu_AAz, including the broad and intense band at ~760 nm, due to the Cu—Cu $\psi \rightarrow \psi^*$ transition [237,238]. Baffling as this result was, collection of an EPR spectrum only confused the matter further, as the EPR spectrum of His120Ala Cu_AAz showed a 4-line hyperfine splitting pattern, suggesting that the site had undergone a transformation to trapped valence (Fig. 10). Adding further confusion, a Q-band ENDOR study of His120Ala Cu_AAz showed evidence for the Cu_A center still being valence delocalized [239].

Recently, Solomon and coworkers were able to finally reconcile the seemingly minimal perturbation imposed by the His120Ala mutation in Cu_AAz, as observed in its UV–vis spectrum, with the drastic change seen in its EPR spectrum, to an apparently trapped-valence species (Fig. 10) [240]. To do this, they applied a series of spectroscopic techniques, including EPR, UV–vis, MCD, RR, and XAS, to both original and His120Ala Cu_AAz, and correlated the results with DFT calculations. The surprising conclusion of this work was that a minute, 1% mixing of the 4s orbital of one copper ion into the ground-state spin wave function caused the collapse to a 4-line hyperfine splitting pattern in the EPR spectrum of His120Ala, *not* a change from valence delocalized to trapped valence. The RR and MCD spectra both demonstrated that the valence delocalization of the Cu_A center was still intact, although slightly perturbed, despite the loss of His120 as a ligand. Solomon and coworkers attributed the ability of Cu_A in azurin to remain valence delocalized, even with the loss of such a strong ligand, to the large electronic coupling matrix element, which arises from the strong and direct Cu—Cu bond. Thus, the diamond core of Cu_A plays an immense role in the robust nature of this center.

If it is truly the diamond core that stabilizes Cu_A and allows it to retain its mixed valence and valence delocalized character, even with the loss of a strong equatorial ligand, then surely any mutation to the diamond core itself, *i.e.* the bridging Cys ligands, would result in significant perturbation to, or loss of, the Cu_A center. Two studies have confirmed this to be true. In the first study, the bridging Cys ligands were individually mutated to Ser [229]. The resulting mutants each bound copper, but in mononuclear types of sites: Cys112Ser in two T2 copper sites, and Cys116Ser in a T1 copper site. Exploring whether the loss of Cu_A formation in these

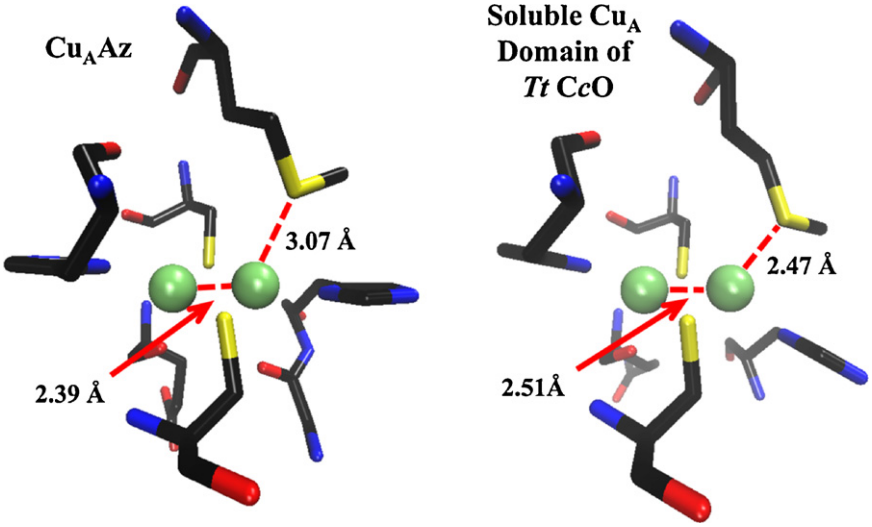

Fig. 9. Cu_A centers of Cu_AAz (left, PDB ID 1CC3) and the soluble Cu_A domain from *Thermus thermophilus* (*Tt*) CcO (right, PDB ID 2CUA), where the Cu—Met and Cu—Cu bond distances are shown. The bond distances given for Cu_AAz are the averages of the distances from two molecules in the asymmetric unit.

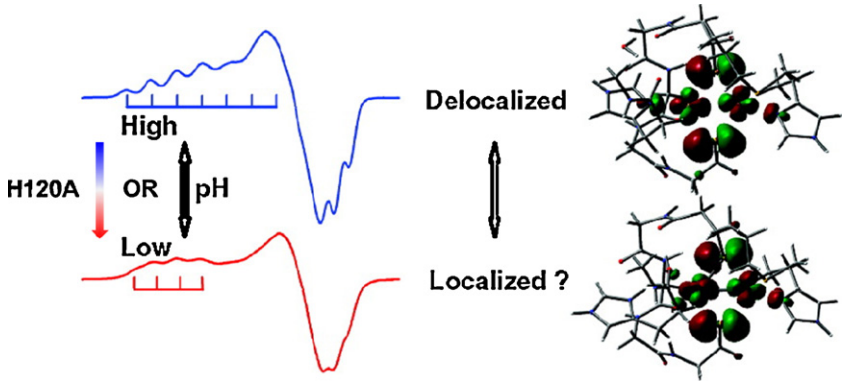

Fig. 10. (Left) Change of 7-line EPR spectrum for original Cu_AAz (top) to 4-line EPR spectrum for His120Ala Cu_AAz (bottom). The same alteration in the EPR spectrum is observed upon transition from high to low pH. (Right) β-LUMOs with the contour values of 0.03 a.u.: (top) high pH 96-atom model and (bottom) low pH 97-atom model [240].

individual Cys mutants was due to loss of symmetry between the bridging ligands, a double Cys to Ser construct was made [241]. At low pH (5.1), this double Cys to Ser mutant bound a single copper ion in a T2 copper site, suggesting that the perturbation to the center due to introduction of the Ser residues was large. However, the pK_a of the Ser alcohol group is much higher than that of the Cys thiol, so metalation of the site at higher pH (8.5) was attempted to see if this would promote binding of two coppers to the site. At pH 8.5, the double Cys to Ser mutant did indeed bind two coppers. EPR analysis, however, showed that the copper ions were in two distinct T2 sites, rather than a mixed valence, Cu_A-like site. Therefore, it is not enough to have symmetry between the bridging ligands, at least when the bridging ligands are alcohols.

3.5. A possible gating mechanism for aerobic respiration regulated by pH-dependent alterations of the Cu_A site

In C*c*O, Cu_A serves as the electron entry point, supplying electrons rapidly and sequentially, first to a low-spin heme *a*, which then passes them on to the catalytic heme–Cu_B site, where the 4 electron reduction of molecular oxygen to water occurs [1,30–32]. This catalytic process is coupled to the pumping of protons across the membrane, creating a potential gradient that drives ATP synthesis. It has been the common belief that a sort of gating mechanism must operate in C*c*O, to activate the system when protons are required, and deactivate the system when enough protons have accumulated. Both the heme–Cu_B catalytic site and the low-spin heme *a* have been proposed to serve as the gate. However, a study of the pH-dependent changes to the Cu_A site in azurin suggests that Cu_A may be this gateway to proton pumping [242].

Gradual adjustment of the pH of fully metalated Cu_AAz results in subtle changes to its UV–vis spectrum. On shifting from pH 4.1 to 6.8, the Cys-S → Cu CT bands decrease slightly, and the Cu—Cu $\psi \rightarrow \psi^*$ transition blue-shifts from ~800 nm to 760 nm. As was observed for His120Ala Cu_AAz, the low pH form of original Cu_AAz displays a 4-line hyperfine splitting pattern in its EPR spectrum, while the high pH form shows the expected 7-line pattern due to valence delocalization. When a protonatable residue was sought out, it was discovered that this pH-dependent behavior was lost in His120Ala Cu_AAz, and moreover, its spectral properties were identical to those of the low pH Cu_AAz. Thus, His120 was assigned as the protonatable residue responsible for this behavior.

Significantly, a 70 mV increase in the reduction potential of the Cu_A center was observed on switching from the high pH, His-on form to the low pH, His-off form. A similar increase of reduction potential has been reported for a number of T1 copper proteins upon protonation of the surface exposed His ligand [243–248]. Under the typical driving forces experienced by Cu_A centers, this change in reduction potential would be enough to essentially halt electron transfer. Therefore, it was proposed, based upon this pH-dependent behavior of the Cu_A in azurin, that Cu_A acts as the gateway for activating and deactivating proton pumping in C*c*O (Fig. 11). Some support for this hypothesis is offered by a mutational study in the Cu_A center of C*c*O from *R. sphaeroides*, where changing the equivalent His residue to Asn causes an ~90 mV increase in the reduction potential of the site, and a decrease in the rate of electron transfer [249,250].

At the same time that Solomon and coworkers did extensive spectroscopic and computational characterization of His120Ala Cu_AAz (see Section 3.4), they also gave the same treatment to both the low- and high-pH forms of Cu_AAz [240]. Thus, the discovery that the 4-line hyperfine splitting pattern in the EPR spectrum of His120Ala Cu_AAz corresponds to a 1% mixing of the 4s orbital of one copper ion into the ground-state spin wavefunction also applies to the low-pH form of original Cu_AAz. In light of this information, Solomon and coworkers sought an explanation for the 2000-fold decrease in the rate of electron transfer observed in a native C*c*O upon transition to low pH, examining each of the variables that could contribute to the decreased rate: reorganization energy, donor–acceptor coupling, and the thermodynamic driving force. Taking into account the known changes to the reorganization energy and the driving force, the rate would be expected to decrease by ~11-fold. This calculation leaves unaccounted for ~180-fold of the observed decrease in the electron transfer rate, which cannot be explained by the donor–acceptor coupling, unless a change occurred in one of the two proposed electron transfer pathways on transition to low pH. In their DFT calculated geometric structure of the low-pH form of Cu_AAz, Solomon and coworkers observed a 0.26 Å increase in the distance between two residues, where a through space jump must occur in one of the electron transfer pathways. As electron tunneling in a through space jump decreases exponentially with increasing distance, this small geometrical change could account for another ~30-fold of the decrease in electron transfer rate. Thus, changes found in the Cu_A center and its electron transfer pathways could account for ~660-fold of the 2000-fold decrease in electron transfer rate from Cu_A to heme *a* in native C*c*Os.

3.6. The advantage of Cu_A revealed by measurement of electron transfer rates for a type 1 copper and Cu_A center in the same protein environment

One major benefit of studying the Cu_AAz biosynthetic model to date was the discovery of an insight it could uniquely offer, which

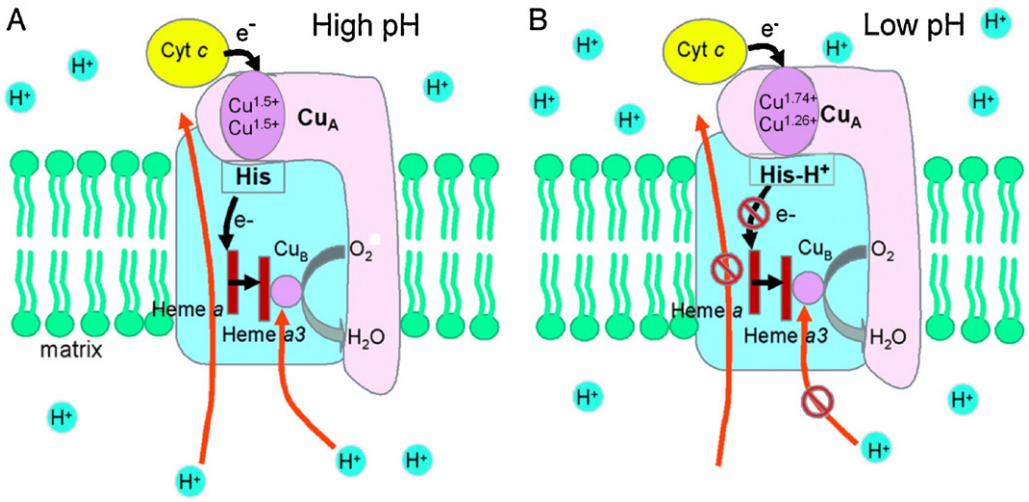

Fig. 11. Schematic depiction of possible proton-pumping gateway function of Cu_A in C*c*O. (A) Under high pH conditions, *i.e.* when few protons have been pumped across the membrane, the Cu_A center is completely valence delocalized, with a reduction potential that enables efficient electron transfer under the operational driving forces. (B) When enough protons have been pumped across the membrane, the Cu_A center becomes 16% less delocalized, and its reduction potential increases by ~70–90 mV, decreasing the efficiency of electron transfer. Solomon and coworkers additionally showed that a conformational change upon transition to low pH shifts the relative positions of two amino acids in one of the electron transfer pathways, which is expected to decrease the electron transfer efficiency by ~30-fold.
Figure adapted from Ref. [242], Copyright 2004 National Academy of Science.

required direct comparison of both a T1 copper center and Cu_A center in the same protein environment. From the time it was learned that Cu_A was a distinct type of site from the T1 copper centers, but one that performed the exact same function, researchers puzzled over why nature had evolved apparently redundant electron transfer centers. Certainly, the T1 copper center was simpler, and as the mechanism of Cu_A formation outlined in Section 3.2 indicates, easier to assemble correctly. Moreover, T1 copper proteins have highly tunable reduction potentials (see Section 2.2), and can easily reach the same reduction potential as Cu_A centers. So why bother with the more complicated and difficult to handle Cu_A? If Cu_A had a functional advantage over T1 copper centers, then this apparently redundant function could be easily explained. However, to demonstrate that such a functional advantage exists, one would have to compare Cu_A and T1 copper sites in the same protein framework, to minimize differences in the electron transfer pathways, donor–acceptor coupling, etc. By nature of its design, Cu_AAz was in a perfect position to settle this conundrum, as the original protein, azurin, contains a T1 copper center in the same location of the protein as the engineered Cu_A. Measurement of the electron transfer rate from a radiolytically reduced disulfide in wtAz and Cu_AAz revealed that, despite a lower driving force, the Cu_A center in Az is more efficient at electron transfer than the T1 copper center [251]. This greater efficiency is due to a lower reorganization energy in Cu_A relative to T1 copper, where the decreased reorganization energy can be explained by the valence delocalization of Cu_A; the geometrical changes wrought by reduction/oxidation are now spread across two copper ions, instead of one. Thus, yet again, the diamond core of Cu_A, with its mixed valence and valence delocalization, determines the remarkable properties of this center.

In another study of the electron transfer rates in Cu_AAz, the apparently trapped-valence low-pH form of Cu_AAz and the corresponding His120Ala variant were compared to valence delocalized original Cu_AAz [252]. The difference in reorganization energy between these two Cu_AAz proteins was only 0.18 eV, much smaller than expected, based on a valence delocalized to trapped-valence transition. At the time, the report from Solomon and coworkers demonstrating that low-pH and His120Ala Cu_AAz were still valence delocalized had not been released. The findings by Solomon and coworkers suggested that the perturbation to the valence delocalization was only 16% [240]. Thus, in light of an only 16% localization of the spin to one copper ion, the 0.18 eV change is actually a sizeable change in reorganization energy, and does reflect the expected contribution of the valence delocalized nature of Cu_A to a low reorganization energy. However, Solomon and coworkers pointed out that a more important factor comes into play at low pH and in the His120Ala variant, which is the binding of an exogenous water ligand in place of His120. This exogenous water ligand should be lost upon reduction, which would be expected to raise the reorganization energy significantly. Again, it seems that the rigid diamond core of Cu_A can rescue its functionality under forces that should be largely perturbing.

4. Conclusions and outlook

Utilization of semi- and fully biosynthetic approaches to study the T1 copper and Cu_A centers in azurin has led to important discoveries about, and showcases of, the nature of these copper-thiolate containing electron transfer centers. In T1 blue copper azurin, incorporation of unnatural amino acids into the protein scaffold has enabled the separation of multiple variables: in one case, the individual contributions of the Cys and Met sulfurs to the covalency of the ground state was elucidated, and in another case, the steric effects of changes in the axial Met ligand were minimized, revealing an underlying hydrophobicity trend in the reduction potentials. Incorporation of the lengthened thiolate ligand, homocysteine, to replace the axial Met, *via* the semi-biosynthetic approach also facilitated a direct demonstration of the coupled distortion theory in a single protein.

The fully biosynthetic Cu_A model, Cu_AAz, has served as an effective springboard for a number of studies which would be difficult to perform in native Cu_A enzymes. Purification of this Cu_A protein in the metal-free form allowed investigation of the *in vitro* assembly of its Cu_A center from addition of Cu(II) alone, from which a unified mechanism of copper incorporation was formulated. Mutagenesis studies of the ligands to the Cu_A center of Cu_AAz have also underscored the importance of the rigid diamond core of Cu_A in maintaining the integrity of this center under perturbing forces,

even the loss of a strong equatorial His ligand. The stability of the Cu_AAz construct over a broad range of pH values has also facilitated elucidation of a possible proton gating function for Cu_A in C*c*O, based on a pH dependent alteration to this center. Finally, the presence of both a T1 copper and Cu_A center in the same protein scaffold of azurin allowed direct comparison of the electron transfer efficiency of these two centers, unearthing the functional advantage of Cu_A: a lower reorganization energy.

As illustrated by the examples discussed in this review, the semi- and fully biosynthetic approaches to studying metalloenzymes can provide unique insights into the properties of native metal centers, which are complementary to the information garnered from top-down and fully synthetic approaches to metalloenzyme studies. While we anticipate that such studies in azurin and Cu_AAz will continue to yield valuable insights, we also look forward to the development of new biosynthetic models for other types of metal centers. Further improvements in computational tools for biosynthetic model design, as well as the ever increasing database of three dimensional protein structures, advances in *de novo* designed proteins, and new ways of incorporating unnatural amino acids will only expedite the development of such biosynthetic metalloenzyme models. Further studies of these biosynthetic models will continue to make significant contributions to understanding the structures and functions of native enzymes and to the construction of artificial redox and ET centers for biotechnological applications.

Acknowledgments

We would like to thank Professor Edward I Solomon for many years of collaboration and inspiration to research in the Lu group, other Lu group members for their contributions to work described in this review, and the US National Science Foundation (award no. CHE-1058959) for financial support.

References

[1] O.M.H. Richter, B. Ludwig, Rev. Physiol. Biochem. Pharmacol. 147 (2003) 47.
[2] W.G. Zumft, P.M.H. Kroneck, in: K.P. Robert (Ed.), Adv. Microb. Physiol., Academic Press, 2006, p. 107.
[3] E.T. Adman, Adv. Protein Chem. 42 (1991) 145.
[4] H.B. Gray, B.G. Malmström, R.J.P. Williams, J. Biol. Inorg. Chem. 5 (2000) 551.
[5] E.I. Solomon, D.W. Randall, T. Glaser, Coord. Chem. Rev. 200–202 (2000) 595.
[6] A.J. Vila, C.O. Fernandez, in: I. Bertini, A. Sigel, H. Sigel (Eds.), Handbook on Metalloproteins, Marcel Dekker, New York, NY, 2001, p. 813.
[7] Y. Lu, in: J.L. Que, W.B. Tolman (Eds.), Biocoordination Chemistry, Elsevier, Oxford, UK, 2004, p. 91.
[8] E.I. Solomon, R.K. Szilagyi, S. DeBeer George, L. Basumallick, Chem. Rev. 104 (2004) 419.
[9] C. Dennison, Coord. Chem. Rev. 249 (2005) 3025.
[10] O. Farver, I. Pecht, Prog. Inorg. Chem., John Wiley & Sons, Inc., 2008, p. 1.
[11] U. Kolczak, C. Dennison, A. Messerschmidt, G.W. Canters, Encyclopedia of Inorganic and Bioinorganic Chemistry, John Wiley & Sons, Ltd., 2011.
[12] E.I. Solomon, J.W. Hare, H.B. Gray, Proc. Natl. Acad. Sci. U.S.A. 73 (1976) 1389.
[13] E.I. Solomon, K.W. Penfield, A.A. Gewirth, M.D. Lowery, S.E. Shadle, J.A. Guckert, L.B. LaCroix, Inorg. Chim. Acta 243 (1996) 67.
[14] J.M. Guss, H.C. Freeman, J. Mol. Biol. 169 (1983) 521.
[15] E.I. Solomon, Inorg. Chem. 45 (2006) 8012.
[16] S.E. Shadle, J.E. Penner-Hahn, H.J. Schugar, B. Hedman, K.O. Hodgson, E.I. Solomon, J. Am. Chem. Soc. 115 (1993) 767.
[17] P.F. Lindley, in: A. Messerschmidt, R. Huber, T. Poulos, K. Wieghardt (Eds.), Handbook of Metalloproteins, Wiley, Chichester, 2001, p. 1369.
[18] M.D. Lowery, J.A. Guckert, M.S. Gebhard, E.I. Solomon, J. Am. Chem. Soc. 115 (1993) 3012.
[19] B.G. Malmström, R. Aasa, FEBS Lett. 325 (1993) 49.
[20] P. Lappalainen, M. Saraste, Biochim. Biophys. Acta: Bioenerg. 1187 (1994) 222.
[21] H. Bertagnolli, W. Kaim, Angew. Chem. Int. Ed. 34 (1995) 771.
[22] T. Tsukihara, H. Aoyama, E. Yamashita, T. Tomizaki, H. Yamaguchi, K. Shinzawa-Itoh, R. Nakashima, R. Yaono, S. Yoshikawa, Science 269 (1995) 1069.
[23] C. Dennison, G.W. Canters, Rec. Trav. Chim. Pays-Bas 115 (1996) 345.
[24] H. Beinert, Eur. J. Biochem. 245 (1997) 521.
[25] D.W. Randall, D.R. Gamelin, L.B. LaCroix, E.I. Solomon, J. Biol. Inorg. Chem. 5 (2000) 16.
[26] J. Sanders-Loehr, in: L.J. Que (Ed.), Physical Methods in Bioinorganic Chemistry, Science Books, Sausalito, 2000, p. 505.
[27] P.M.H. Kroneck, in: A. Messerschmidt, R. Huber, T. Poulos, K. Wieghardt (Eds.), Handbook of Metalloproteins, Wiley, Chichester, 2001, p. 1333.
[28] M.G. Savelieff, Y. Lu, J. Biol. Inorg. Chem. 15 (2010) 461.
[29] S. Iwata, C. Ostermeier, B. Ludwig, H. Michel, Nature 376 (1995) 660.
[30] M. Wikstrom, Biochim. Biophys. Acta 1655 (2004) 241.
[31] M. Brunori, A. Giuffre, P. Sarti, J. Inorg. Biochem. 99 (2005) 324.
[32] P. Brzezinski, R.B. Gennis, J. Bioenerg. Biomembr. 40 (2008) 521.
[33] K. Brown, M. Tegoni, M. Prudencio, A.S. Pereira, S. Besson, J.J. Moura, I. Moura, C. Cambillau, Nat. Struct. Biol. 7 (2000) 191.
[34] T. Haltia, K. Brown, M. Tegoni, C. Cambillau, M. Saraste, K. Mattila, K. Djinovic-Carugo, J. Biochem. 369 (2003) 77.
[35] W.G. Zumft, P.M. Kroneck, Adv. Microb. Physiol. 52 (2007) 107.
[36] Suharti, M.J. Strampraad, I. Schröder, S. de Vries, Biochemistry 40 (2001) 2632.
[37] Suharti, H.A. Heering, S. de Vries, Biochemistry 43 (2004) 13487.
[38] L. Komorowski, S. Anemuller, G. Schafer, J. Bioenerg. Biomembr. 33 (2001) 27.
[39] L. Komorowski, W. Verheyen, G. Schafer, Biol. Chem. 383 (2002) 1791.
[40] T. Tsukihara, H. Aoyama, E. Yamashita, T. Tomizaki, H. Yamaguchi, K. Shinzawa-Itoh, R. Nakashima, R. Yaono, S. Yoshikawa, Science 272 (1996) 1136.
[41] K. Brown, K. Djinovic-Carugo, T. Haltia, I. Cabrito, M. Saraste, J.J. Moura, I. Moura, M. Tegoni, C. Cambillau, J. Biol. Chem. 275 (2000) 41133.
[42] K. Paraskevopoulos, S.V. Antonyuk, R.G. Sawers, R.R. Eady, S.S. Hasnain, J. Mol. Biol. 362 (2006) 55.
[43] N.J. Blackburn, M.E. Barr, W.H. Woodruff, J. van der Ooost, S. de Vries, Biochemistry 33 (1994) 10401.
[44] G. Henkel, A. Müller, S. Weissgräber, G. Buse, T. Soulimane, G.C.M. Steffens, H.-F. Nolting, Angew. Chem. Int. Ed. 34 (1995) 1488.
[45] L.G. Ryden, L.T. Hunt, J. Mol. Evol. 36 (1993) 41.
[46] B. Abolmaali, H. Taylor, U. Weser, in: M. Clarke, J. Goodenough, C. Jørgensen, D. Mingos, G. Palmer, P. Sadler, R. Weiss, R. Williams (Eds.), Structure & Bonding, Springer, Berlin/Heidelberg, 1998, p. 91.
[47] R.P. Amber, J. Chem. Soc. Pak. 21 (1999) 213.
[48] D.R. Gamelin, D.W. Randall, M.T. Hay, R.P. Houser, T.C. Mulder, G.W. Canters, S. de Vries, W.B. Tolman, Y. Lu, E.I. Solomon, J. Am. Chem. Soc. 120 (1998) 5246.
[49] F. Neese, W.G. Zumft, W.E. Antholine, P.M.H. Kroneck, J. Am. Chem. Soc. 118 (1996) 8692.
[50] J.A. Farrar, F. Neese, P. Lappalainen, P.M.H. Kroneck, M. Saraste, W.G. Zumft, A.J. Thomson, J. Am. Chem. Soc. 118 (1996) 11501.
[51] P.M. Kroneck, W.E. Antholine, H. Koteich, D.H.W. Kastrau, F. Neese, W.G. Zumft, in: K.D. Karlin, Z. Tyeklár (Eds.), Bioinorganic Chemistry of Copper, Chapman & Hall, New York, NY, 1993, p. 419.
[52] W.E. Antholine, D.H. Kastrau, G.C. Steffens, G. Buse, W.G. Zumft, P.M. Kroneck, Eur. J. Biochem. 209 (1992) 875.
[53] M.H.M. Olsson, U. Ryde, J. Am. Chem. Soc. 123 (2001) 7866.
[54] E.I. Solomon, X. Xie, A. Dey, Chem. Soc. Rev. 37 (2008) 623.
[55] J. Riester, W.G. Zumft, P.M. Kroneck, Eur. J. Biochem. 178 (1989) 751.
[56] C.L. Hulse, B.A. Averill, Biochem. Biophys. Res. Commun. 166 (1990) 729.
[57] P. Lappalainen, R. Aasa, B.G. Malmstrom, M. Saraste, J. Biol. Chem. 268 (1993) 26416.
[58] C. von Wachenfeldt, S. de Vries, J. van der Oost, FEBS Lett. 340 (1994) 109.
[59] C.E. Slutter, D. Sanders, P. Wittung, B.G. Malmstrom, R. Aasa, J.H. Richards, H.B. Gray, J.A. Fee, Biochemistry 35 (1996) 3387.
[60] P.A. Williams, N.J. Blackburn, D. Sanders, H. Bellamy, E.A. Stura, J.A. Fee, D.E. McRee, Nat. Struct. Biol. 6 (1999) 509.
[61] A.X. Song, L.Z. Li, T. Yu, S.M. Chen, Z.X. Huang, Protein Eng. 16 (2003) 435.
[62] M. Paumann, B. Lubura, G. Regelsberger, M. Feichtinger, G. Kollensberger, C. Jakopitsch, P.G. Furtmuller, G.A. Peschek, C. Obinger, J. Biol. Chem. 279 (2004) 10293.
[63] W. Froncisz, C.P. Scholes, J.S. Hyde, Y.H. Wei, T.E. King, R.W. Shaw, H. Beiner, J. Biol. Chem. 254 (1979) 7482.
[64] B.M. Hoffman, J.E. Roberts, M. Swanson, S.H. Speck, E. Margoliash, Proc. Natl. Acad. Sci. U.S.A. 77 (1980) 1452.
[65] C.E. Slutter, I. Gromov, J.H. Richards, I. Pecht, D. Goldfarb, J. Am. Chem. Soc. 121 (1999) 5077.
[66] J.A. Farrar, P. Lappalainen, W.G. Zumft, M. Saraste, A.J. Thomson, Eur. J. Biochem. 232 (1995) 294.
[67] P. Lappalainen, N.J. Watmough, C. Greenwood, M. Saraste, Biochemistry 34 (1995) 5824.
[68] C.E. Slutter, R. Langen, D. Sanders, S.M. Lawrence, P. Wittung, A.J. Di Bilio, M.G. Hill, J.A. Fee, J.H. Richards, J.R. Winkler, B.G. Malmström, Inorg. Chim. Acta 243 (1996) 141.
[69] O. Maneg, B. Ludwig, F. Malatesta, J. Biol. Chem. 278 (2003) 46734.
[70] J. van der Oost, P. Lappalainen, A. Musacchio, A. Warne, L. Lemieux, J. Rumbley, R.B. Gennis, R. Aasa, T. Pascher, B.G. Malmstrom, et al., EMBO J. 11 (1992) 3209.
[71] C. Dennison, E. Vijgenboom, S. de Vries, J. van der Oost, G.W. Canters, FEBS Lett. 365 (1995) 92.
[72] M. Hay, J.H. Richards, Y. Lu, Proc. Natl. Acad. Sci. U.S.A. 93 (1996) 461.
[73] L.H. Jones, A. Liu, V.L. Davidson, J. Biol. Chem. 278 (2003) 47269.
[74] C. Immoos, M.G. Hill, D. Sanders, J.A. Fee, C.E. Slutter, J.H. Richards, H.B. Gray, J. Biol. Inorg. Chem. 1 (1996) 529.
[75] K. Fujita, N. Nakamura, H. Ohno, B.S. Leigh, K. Niki, H.B. Gray, J.H. Richards, J. Am. Chem. Soc. 126 (2004) 13954.
[76] G.N. Ledesma, D.H. Murgida, H.K. Ly, H. Wackerbarth, J. Ulstrup, A.J. Costa-Filho, A.J. Vila, J. Am. Chem. Soc. 129 (2007) 11884.
[77] C. Belle, W. Rammal, J.-L. Pierre, J. Inorg. Biochem. 99 (2005) 1929.

[78] R.H. Holm, E.I. Solomon, Chem. Rev. 104 (2004) 347.
[79] C. Harding, V. McKee, J. Nelson, J. Am. Chem. Soc. 113 (1991) 9684.
[80] M.E. Barr, P.H. Smith, W.E. Antholine, B. Spencer, J. Chem. Soc. Chem. Commun. (1993) 1649.
[81] C. Harding, J. Nelson, M.C.R. Symons, J. Wyatt, J. Chem. Soc. Chem. Commun. (1994) 2499.
[82] R.P. Houser, W.B. Tolman, Inorg. Chem. 34 (1995) 1632.
[83] R.P. Houser, V.G. Young, W.B. Tolman, J. Am. Chem. Soc. 118 (1996) 2101.
[84] D.D. LeCloux, R. Davydov, S.J. Lippard, J. Am. Chem. Soc. 120 (1998) 6810.
[85] H.W. Yim, L.M. Tran, E.E. Pullen, D. Rabinovich, L.M. Liable-Sands, T.E. Concolino, A.L. Rheingold, Inorg. Chem. 38 (1999) 6234.
[86] V.M. Miskowski, S. Franzen, A.P. Shreve, M.R. Ondrias, S.E. Wallace-Williams, M.E. Barr, W.H. Woodruff, Inorg. Chem. 38 (1999) 2546.
[87] C. He, S.J. Lippard, Inorg. Chem. 39 (2000) 5225.
[88] S. Franzen, V.M. Miskowski, A.P. Shreve, S.E. Wallace-Williams, W.H. Woodruff, M.R. Ondrias, M.E. Barr, L. Moore, S.G. Boxer, Inorg. Chem. 40 (2001) 6375.
[89] R. Gupta, Z.H. Zhang, D. Powell, M.P. Hendrich, A.S. Borovik, Inorg. Chem. 41 (2002) 5100.
[90] S.B. Harkins, J.C. Peters, J. Am. Chem. Soc. 126 (2004) 2885.
[91] Q. Zhao, X. Wang, Y. Liu, R. Fang, Chem. Lett. 33 (2004) 138.
[92] Y.-H. Wen, J.-K. Cheng, J. Zhang, Z.-J. Li, Y. Kang, Y.-G. Yao, Inorg. Chem. Commun. 7 (2004) 1120.
[93] D.V. Patel, D.J. Mihalcik, K.A. Kreisel, G.P.A. Yap, L.N. Zakharov, W.S. Kassel, A.L. Rheingold, D. Rabinovich, Dalton Trans. (2005) 2410.
[94] Y. Feng, Z. Han, J. Peng, X. Hao, J. Mol. Struct. 734 (2005) 171.
[95] X. Jiang, J.C. Bollinger, M.-H. Baik, D. Lee, Chem. Commun. (2005) 1043.
[96] S. Kababya, J. Nelson, C. Calle, F. Neese, D. Goldfarb, J. Am. Chem. Soc. 128 (2006) 2017.
[97] F. Muh, A. Zouni, Front. Biosci. Landmark Ed. 16 (2011) 3072.
[98] A.S. Hakemian, A.C. Rosenzweig, Annu. Rev. Biochem. 76 (2007) 223.
[99] V. Nanda, R.L. Koder, Nat. Chem. 2 (2010) 15.
[100] N. Sailasuta, F.C. Anson, H.B. Gray, J. Am. Chem. Soc. 101 (1979) 455.
[101] A.G. Mauk, G.R. Moore, J. Biol. Inorg. Chem. 2 (1997) 119.
[102] A. Warshel, A. Papazyan, I. Muegge, J. Biol. Inorg. Chem. 2 (1997) 143.
[103] M.K. Eidsness, A.E. Burden, K.A. Richie, D.M. Kurtz, R.A. Scott, E.T. Smith, T. Ichiye, B. Beard, T. Min, C. Kang, Biochemistry 38 (1999) 14803.
[104] D.W. Low, M.G. Hill, J. Am. Chem. Soc. 120 (1998) 11536.
[105] F. Capozzi, S. Ciurli, C. Luchinat, in: H. Hill, P. Sadler, A. Thomson (Eds.), Structure & Bonding, Springer, Berlin/Heidelberg, 1998, p. 127.
[106] I. Bertini, G. Gori-Savellini, C. Luchinat, J. Biol. Inorg. Chem. 2 (1997) 114.
[107] B. Shen, D.R. Jollie, C.D. Stout, T.C. Diller, F.A. Armstrong, C.M. Gorst, G.N. La Mar, P.J. Stephens, B.K. Burgess, J. Biol. Chem. 269 (1994) 8564.
[108] A. Dey, F.E. Jenney, M.W. Adams Jr., E. Babini, Y. Takahashi, K. Fukuyama, K.O. Hodgson, B. Hedman, E.I. Solomon, Science 318 (2007) 1464.
[109] G. Backes, Y. Mino, T.M. Loehr, T.E. Meyer, M.A. Cusanovich, W.V. Sweeney, E.T. Adman, J. Sanders-Loehr, J. Am. Chem. Soc. 113 (1991) 2055.
[110] X. Yang, S. Niu, T. Ichiye, L.-S. Wang, J. Am. Chem. Soc. 126 (2004) 15790.
[111] E. Adman, K.D. Watenpaugh, L.H. Jensen, Proc. Natl. Acad. Sci. U.S.A. 72 (1975) 4854.
[112] S. Niu, T. Ichiye, J. Am. Chem. Soc. 131 (2009) 5724.
[113] P.D. Swartz, B.W. Beck, T. Ichiye, Biophys. J. 71 (1996) 2958.
[114] P.D. Swartz, T. Ichiye, Biophys. J. 73 (1997) 2733.
[115] P.J. Stephens, D.R. Jollie, A. Warshel, Chem. Rev. 96 (1996) 2491.
[116] D.S. Cohen, G.J. Pielak, J. Am. Chem. Soc. 117 (1995) 1675.
[117] S. Benini, M. Borsari, S. Ciurli, A. Dikiy, M. Lamborghini, J. Biol. Inorg. Chem. 3 (1998) 371.
[118] G. Battistuzzi, L. Loschi, M. Borsari, M. Sola, J. Biol. Inorg. Chem. 4 (1999) 601.
[119] R. Varadarajan, T.E. Zewert, H.B. Gray, S.G. Boxer, Science 243 (1989) 69.
[120] M.R. Gunner, E. Alexov, E. Torres, S. Lipovaca, J. Biol. Inorg. Chem. 2 (1997) 126.
[121] M.H.M. Olsson, G. Hong, A. Warshel, J. Am. Chem. Soc. 125 (2003) 5025.
[122] A. Donaire, B. Jimenez, J. Moratal, J.F. Hall, S.S. Hasnain, Biochemistry 40 (2001) 837.
[123] M.C. Machczynski, H.B. Gray, J.H. Richards, J. Inorg. Biochem. 88 (2002) 375.
[124] S. Yanagisawa, K. Sato, M. Kikuchi, T. Kohzuma, C. Dennison, Biochemistry 42 (2003) 6853.
[125] C. Fernández, T. Niizeki, T. Kohzuma, A. Vila, J. Biol. Inorg. Chem. 8 (2003) 75.
[126] G. Battistuzzi, M. Borsari, L. Loschi, M. Sola, J. Biol. Inorg. Chem. 2 (1997) 350.
[127] G. Battistuzzi, M. Borsari, L. Loschi, M. Sola, J. Inorg. Biochem. 69 (1998) 97.
[128] G. Battistuzzi, M. Borsari, J.A. Cowan, C. Eicken, L. Loschi, M. Sola, Biochemistry 38 (1999) 5553.
[129] G. Battistuzzi, M. Borsari, L. Loschi, A. Ranieri, M. Sola, B. Mondovi, A. Marchesini, J. Inorg. Biochem. 83 (2001) 223.
[130] G. Battistuzzi, M. Borsari, L. Loschi, M.C. Menziani, R.F. De, M. Sola, Biochemistry 40 (2001) 6422.
[131] G. Battistuzzi, M. Borsari, G.W. Canters, W.E. de, L. Loschi, G. Warmerdam, M. Sola, Biochemistry 40 (2001) 6707.
[132] N.M. Marshall, D.K. Garner, T.D. Wilson, Y.-G. Gao, H. Robinson, M.J. Nilges, Y. Lu, Nature 462 (2009) 113.
[133] S.M. Berry, E.L. Bladholm, E.J. Mostad, A.R. Schenewerk, J. Biol. Inorg. Chem. 16 (2011) 473.
[134] P. Zheng, S.-i.J. Takayama, A.G. Mauk, H. Li, J. Am. Chem. Soc. 134 (2012) 4124.
[135] Y.-C. Liu, L.-K. Tu, T.-H. Yen, G.-H. Lee, S.-T. Yang, M.-H. Chiang, Inorg. Chem. 49 (2010) 6409.
[136] A.S. Borovik, Acc. Chem. Res. 38 (2004) 54.
[137] R.L. Shook, A.S. Borovik, Chem. Commun. 14 (2008) 6095.
[138] R.L. Shook, A.S. Borovik, Inorg. Chem. 49 (2010) 3646.
[139] Y. Lu, S.M. Berry, T.D. Pfister, Chem. Rev. 101 (2001) 3047.
[140] Y. Lu, Curr. Opin. Chem. Biol. 9 (2005) 118.
[141] Y. Lu, Angew. Chem. Int. Ed. 45 (2006) 5588.
[142] Y. Lu, N. Yeung, N. Sieracki, N.M. Marshall, Nature 460 (2009) 855.
[143] D. Ghosh, V.L. Pecoraro, Inorg. Chem. 43 (2004) 7902.
[144] D. Ghosh, V.L. Pecoraro, Curr. Opin. Chem. Biol. 9 (2005) 97.
[145] J.R. Calhoun, F. Nastri, O. Maglio, V. Pavone, A. Lombardi, W.F. DeGrado, Biopolymers 80 (2005) 264.
[146] O. Maglio, F. Nastri, d.R. Martin, Rafael Torres, M. Faiella, V. Pavone, W.F. DeGrado, A. Lombardi, C.R. Chim. 10 (2007) 703.
[147] A.F.A. Peacock, O. Iranzo, V.L. Pecoraro, Dalton Trans. (2009) 2271.
[148] F. Rosati, G. Roelfes, ChemCatChem 2 (2010) 916.
[149] M.L. Zastrow, A.F.A. Peacock, J.A. Stuckey, V.L. Pecoraro, Nat. Chem. 4 (2012) 118.
[150] L. Banci, Curr. Opin. Chem. Biol. 7 (2003) 143.
[151] G. Böhm, Biophys. Chem. 59 (1996) 1.
[152] E.H. Lee, J. Hsin, M. Sotomayor, G. Comellas, K. Schulten, Structure 17 (2009) 1295.
[153] K.M. Clark, W.A. van der Donk, Y. Lu, in: W.M. Tom, N.A. John (Eds.), Methods Enzymol., Academic Press, 2009, p. 97.
[154] B.G. Karlsson, M. Nordling, T. Pascher, L.-C. Tsai, L. Sjolin, L.G. Lundberg, Protein Eng. 4 (1991) 343.
[155] T. Den Blaauwen, M. Van de Kamp, G.W. Canters, J. Am. Chem. Soc. 113 (1991) 5050.
[156] T. Den Blaauwen, G.W. Canters, J. Am. Chem. Soc. 115 (1993) 1121.
[157] T.J. Mizoguchi, A.J. Di Bilio, H.B. Gray, J.H. Richards, J. Am. Chem. Soc. 114 (1992) 10076.
[158] M. Piccioli, C. Luchinat, T.J. Mizoguchi, B.E. Ramirez, H.B. Gray, J.H. Richards, Inorg. Chem. 34 (1995) 737.
[159] S. Faham, T.J. Mizoguchi, E.T. Adman, H.B. Gray, J.H. Richards, D.C. Rees, J. Biol. Inorg. Chem. 2 (1997) 464.
[160] S. DeBeer, C.N. Kiser, G.A. Mines, J.H. Richards, H.B. Gray, E.I. Solomon, B. Hedman, K.O. Hodgson, Inorg. Chem. 38 (1999) 433.
[161] K.M. Lancaster, S.D. George, K. Yokoyama, J.H. Richards, H.B. Gray, Nat. Chem. 1 (2009) 711.
[162] K.M. Lancaster, K. Yokoyama, J.H. Richards, J.R. Winkler, H.B. Gray, Inorg. Chem. 48 (2009) 1278.
[163] K.M. Lancaster, S. Sproules, J.H. Palmer, J.H. Richards, H.B. Gray, J. Am. Chem. Soc. 132 (2010) 14590.
[164] K.M. Lancaster, O. Farver, S. Wherland, E.J. Crane, J.H. Richards III, I. Pecht, H.B. Gray, J. Am. Chem. Soc. 133 (2011) 4865.
[165] S.B.H. Kent, Chem. Soc. Rev. 38 (2009) 338.
[166] P.E. Dawson, T.W. Muir, I. Clark-Lewis, S.B. Kent, Science 266 (1994) 776.
[167] T.W. Muir, D. Sondhi, P.a. Cole, Proc. Natl. Acad. Sci. U.S.A. 95 (1998) 6705.
[168] L. Wang, a. Brock, B. Herberich, P.G. Schultz, Science 292 (2001) 498.
[169] C.C. Liu, P.G. Schultz, Annu. Rev. Biochem. 79 (2010) 413.
[170] T.C. Evans, J. Benner Jr., M.Q. Xu, Protein Sci. 7 (1998) 2256.
[171] B. Ayers, U.K. Blaschke, J.A. Camarero, G.J. Cotton, M. Holford, T.W. Muir, Biopolymers 51 (1999) 343.
[172] S.M. Berry, M.D. Gieselman, M.J. Nilges, W.A. van der Donk, Y. Lu, J. Am. Chem. Soc. 124 (2002) 2084.
[173] S.M. Berry, M. Ralle, D.W. Low, N.J. Blackburn, Y. Lu, J. Am. Chem. Soc. 125 (2003) 8760.
[174] M. Ralle, S.M. Berry, M.J. Nilges, M.D. Gieselman, W.A. van der Donk, Y. Lu, N.J. Blackburn, J. Am. Chem. Soc. 126 (2004) 7244.
[175] D.K. Garner, M.D. Vaughan, H.J. Hwang, M.G. Savelieff, S.M. Berry, J.F. Honek, Y. Lu, J. Am. Chem. Soc. 128 (2006) 15608.
[176] K.M. Clark, Y. Yu, N.M. Marshall, N.A. Sieracki, M.J. Nilges, N.J. Blackburn, W.A. van der Donk, Y. Lu, J. Am. Chem. Soc. 132 (2010) 10093.
[177] R. Sarangi, S.I. Gorelsky, L. Basumallick, H.J. Hwang, R.C. Pratt, T.D.P. Stack, Y. Lu, K.O. Hodgson, B. Hedman, E.I. Solomon, J. Am. Chem. Soc. 130 (2008) 3866.
[178] T. Pascher, B.G. Karlsson, M. Nordling, B.G. Malmstrom, T. Vanngard, Eur. J. Biochem. 212 (1993) 289.
[179] S.J. Kroes, C.W.G. Hoitink, C.R. Andrew, J. Sanders-Loehr, A. Messerschmidt, W.R. Hagen, G.W. Canters, Eur. J. Biochem. 240 (1996) 342.
[180] L.M. Murphy, R.W. Strange, B.G. Karlsson, L.G. Lundberg, T. Pascher, B. Reinhammar, S.S. Hasnain, Biochemistry 32 (1993) 1965.
[181] N. Bonander, B.G. Karlsson, T. Vanngard, Biochemistry 35 (1996) 2429.
[182] L.C. Tsai, N. Bonander, K. Harata, G. Karlsson, T. Vanngard, V. Langer, L. Sjolin, Acta Crystallogr. D: Biol. Crystallogr. 52 (1996) 950.
[183] O. Farver, L.K. Skov, T. Pascher, B.G. Karlsson, M. Nordling, L.G. Lundberg, T. Vanngard, I. Pecht, Biochemistry 32 (1993) 7317.
[184] R. Bauer, E. Danielsen, L. Hemmingsen, M.J. Bjerrum, Ö. Hansson, K. Singh, J. Am. Chem. Soc. 119 (1997) 157.
[185] J. Salgado, S.J. Kroes, A. Berg, J.M. Moratal, G.W. Canters, J. Biol. Chem. 273 (1998) 177.
[186] S. DeBeer, D.W. Randall, A.M. Nersissian, J.S. Valentine, B. Hedman, K.O. Hodgson, E.I. Solomon, J. Phys. Chem. B 104 (2000) 10814.
[187] Y. Lu, L.B. LaCroix, M.D. Lowery, E.I. Solomon, C.J. Bender, J. Peisach, J.A. Roe, E.B. Gralla, J.S. Valentine, J. Am. Chem. Soc. 115 (1993) 5907.
[188] J. Han, T.M. Loehr, Y. Lu, J.S. Valentine, B.A. Averill, J. Sanders-Loehr, J. Am. Chem. Soc. 115 (1993) 4256.
[189] L.B. LaCroix, S.E. Shadle, Y. Wang, B.A. Averill, B. Hedman, K.O. Hodgson, E.I. Solomon, J. Am. Chem. Soc. 118 (1996) 7755.

Please cite this article in press as: T.D. Wilson, et al., Coord. Chem. Rev. (2012), http://dx.doi.org/10.1016/j.ccr.2012.06.015

[190] A. Messerschmidt, L. Prade, S.J. Kroes, J. Sanders-Loehr, R. Huber, G.W. Canters, Proc. Natl. Acad. Sci. U.S.A. 95 (1998) 3443.
[191] L.B. LaCroix, D.W. Randall, A.M. Nersissian, C.W.G. Hoitink, G.W. Canters, J.S. Valentine, E.I. Solomon, J. Am. Chem. Soc. 120 (1998) 9621.
[192] A.E. Palmer, D.W. Randall, F. Xu, E.I. Solomon, J. Am. Chem. Soc. 121 (1999) 7138.
[193] D.W. Randall, S.D. George, P.L. Holland, B. Hedman, K.O. Hodgson, W.B. Tolman, E.I. Solomon, J. Am. Chem. Soc. 122 (2000) 11632.
[194] P. Frank, A. Licht, T.D. Tullius, K.O. Hodgson, I. Pecht, J. Biol. Chem. 260 (1985) 5518.
[195] D.M. Arciero, A.B. Hooper, A.C. Rosenzweig, Biochemistry 40 (2001) 5674.
[196] B.S. Pierce, M.P. Hendrich, A.B. Hooper, Biochemistry 41 (2002) 1703.
[197] L. Basumallick, R. Sarangi, S. DeBeer George, B. Elmore, A.B. Hooper, B. Hedman, K.O. Hodgson, E.I. Solomon, J. Am. Chem. Soc. 127 (2005) 3531.
[198] M. van Gestel, G.W. Canters, H. Krupka, A. Messerschmidt, E.C. de Waal, G.C.M. Warmerdam, E.J.J. Groenen, J. Am. Chem. Soc. 122 (2000) 2322.
[199] B.G. Karlsson, L.-C. Tsai, H. Nar, J. Sanders-Loehr, N. Bonander, V. Langer, L. Sjolin, Biochemistry 36 (1997) 4089.
[200] R.W. Strange, L.M. Murphy, B.G. Karlsson, B. Reinhammar, S.S. Hasnain, Biochemistry 35 (1996) 16391.
[201] M.A. Webb, C.N. Kiser, J.H. Richards, A.J. Di Bilio, H.B. Gray, J.R. Winkler, G.R. Loppnow, J. Phys. Chem. B 104 (2000) 10915.
[202] L. Basumallick, R.K. Szilagyi, Y. Zhao, J.P. Shapleigh, C.P. Scholes, E.I. Solomon, J. Am. Chem. Soc. 125 (2003) 14784.
[203] C.R. Andrew, P. Lappalainen, M. Saraste, M.T. Hay, Y. Lu, C. Dennison, G.W. Canters, J.A. Fee, N. Nakamura, J. Sanders-Loehr, J. Am. Chem. Soc. 117 (1995) 10759.
[204] M.T. Hay, M.C. Ang, D.R. Gamelin, E.I. Solomon, W.E. Antholine, M. Ralle, N.J. Blackburn, P.D. Massey, X. Wang, A.H. Kwon, Y. Lu, Inorg. Chem. 37 (1998) 191.
[205] S. DeBeer George, M. Metz, R.K. Szilagyi, H. Wang, S.P. Cramer, Y. Lu, W.B. Tolman, B. Hedman, K.O. Hodgson, E.I. Solomon, J. Am. Chem. Soc. 123 (2001) 5757.
[206] B. Epel, C.S. Slutter, F. Neese, P.M.H. Kroneck, W.G. Zumft, I. Pecht, O. Farver, Y. Lu, D. Goldfarb, J. Am. Chem. Soc. 124 (2002) 8152.
[207] H. Robinson, M.C. Ang, Y.-G. Gao, M.T. Hay, Y. Lu, A.H.J. Wang, Biochemistry 38 (1999) 5677.
[208] B.-E. Kim, T. Nevitt, D.J. Thiele, Nat. Chem. Biol. 4 (2008) 176.
[209] S.C. Leary, D.R. Winge, P.A. Cobine, Biochim. Biophys. Acta 1793 (2009) 146.
[210] A.K. Boal, A.C. Rosenzweig, Chem. Rev. 109 (2009) 4760.
[211] L. Banci, I. Bertini, K.S. McGreevy, A. Rosato, Nat. Prod. Rep. 27 (2010).
[212] N.J. Robinson, D.R. Winge, Annu. Rev. Biochem. 79 (2010) 537.
[213] I. Bertini, G. Cavallaro, K.S. McGreevy, Coord. Chem. Rev. 254 (2010) 506.
[214] L. Banci, I. Bertini, F. Cantini, S. Ciofi-Baffoni, Cell. Mol. Life Sci. 67 (2010) 2563.
[215] L. Banci, I. Bertini, G. Cavallaro, S. Ciofi-Baffoni, FEBS J. 278 (2011) 2244.
[216] C. Ostermeier, S. Iwata, B. Ludwig, H. Michel, Nat. Struct. Biol. 2 (1995) 842.
[217] T. Soulimane, G. Buse, G.P. Bourenkov, H.D. Bartunik, R. Huber, M.E. Than, EMBO J. 19 (2000) 1766.
[218] W.G. Zumft, Microbiol. Mol. Biol. Rev. 61 (1997) 533.
[219] P. Wunsch, M. Herb, H. Wieland, U.M. Schiek, W.G. Zumft, J. Bacteriol. 185 (2003) 887.
[220] W.G. Zumft, J. Mol. Microbiol. Biotechnol. 10 (2005) 154.
[221] D.E. Davidson, B.C. Hill, Biochim. Biophys. Acta 1794 (2009) 275.
[222] G.S. Siluvai, M.M. Nakano, M. Mayfield, M.J. Nilges, N.J. Blackburn, Biochemistry 48 (2009) 12133.
[223] G. Siluvai, M. Nakano, M. Mayfield, N. Blackburn, J. Biol. Inorg. Chem. 16 (2011) 285.
[224] X. Wang, M.C. Ang, Y. Lu, J. Am. Chem. Soc. 121 (1999) 2947.
[225] D. Cavallini, C. De Marco, S. Dupre, Arch. Biochem. Biophys. 124 (1968) 18.
[226] D. Cavallini, C. De Marco, S. Dupre, G. Rotilio, Arch. Biochem. Biophys. 130 (1969) 354.
[227] L. Pecci, G. Montefoschi, G. Musci, D. Cavallini, Amino Acids 13 (1997) 355.
[228] T.D. Wilson, M.G. Savelieff, M.J. Nilges, N.M. Marshall, Y. Lu, J. Am. Chem. Soc. 133 (2011) 20778.
[229] H.J. Hwang, N. Nagraj, Y. Lu, Inorg. Chem. 45 (2006) 102.
[230] W. Maret, H. Kozlowski, Biochim. Biophys. Acta 912 (1987) 329.
[231] J.A. Farrar, G. Formicka, M. Zeppezauer, A.J. Thomson, Biochem. J. 317 (Pt 2) (1996) 447.
[232] W. Maret, H. Dietrich, H.H. Ruf, M. Zeppezauer, J. Inorg. Biochem. 12 (1980) 241.
[233] W. Maret, M. Zeppezauer, A. Desideri, L. Morpurgo, G. Rotilio, FEBS Lett. 136 (1981) 72.
[234] A. Holmgren, J. Biol. Chem. 264 (1989) 13963.
[235] J. Nordberg, E.S. Arner, Free Radical Bio. Med. 31 (2001) 1287.
[236] H.J. Hwang, S.M. Berry, M.J. Nilges, Y. Lu, J. Am. Chem. Soc. 127 (2005) 7274.
[237] X. Wang, S.M. Berry, Y. Xia, Y. Lu, J. Am. Chem. Soc. 121 (1999) 7449.
[238] S.M. Berry, X. Wang, Y. Lu, J. Inorg. Biochem. 78 (2000) 89.
[239] D. Lukoyanov, S.M. Berry, Y. Lu, W.E. Antholine, C.P. Scholes, Biophys. J. 82 (2002) 2758.
[240] X. Xie, S.I. Gorelsky, R. Sarangi, D.K. Garner, H.J. Hwang, K.O. Hodgson, B. Hedman, Y. Lu, E.I. Solomon, J. Am. Chem. Soc. 130 (2008) 5194.
[241] M.G. Savelieff, Y. Lu, Inorg. Chim. Acta 361 (2008) 1087.
[242] H.J. Hwang, Y. Lu, Proc. Natl. Acad. Sci. U.S.A. 101 (2004) 12842.
[243] A.G. Sykes, Chem. Soc. Rev. 14 (1985) 283.
[244] J.M. Guss, P.R. Harrowell, M. Murata, V.A. Norris, H.C. Freeman, J. Mol. Biol. 192 (1986) 361.
[245] A. Lommen, G.W. Canters, J. van Beeumen, Eur. J. Biochem. 176 (1988) 213.
[246] A. Lommen, G.W. Canters, J. Biol. Chem. 265 (1990) 2768.
[247] C. Dennison, T. Kohzuma, W. McFarlane, S. Suzuki, A.G. Sykes, Inorg. Chem. 33 (1994) 3299.
[248] L.J.C. Jeuken, P. van Vliet, M.P. Verbeet, R. Camba, J.P. McEvoy, F.A. Armstrong, G.W. Canters, J. Am. Chem. Soc. 122 (2000) 12186.
[249] Y. Zhen, B. Schmidt, U.G. Kang, W. Antholine, S. Ferguson-Miller, Biochemistry 41 (2002) 2288.
[250] K. Wang, L. Geren, Y. Zhen, L. Ma, S. Ferguson-Miller, B. Durham, F. Millett, Biochemistry 41 (2002) 2298.
[251] O. Farver, Y. Lu, M.C. Ang, I. Pecht, Proc. Natl. Acad. Sci. U.S.A. 96 (1999) 899.
[252] O. Farver, H.J. Hwang, Y. Lu, I. Pecht, J. Phys. Chem. B 111 (2007) 6690.

Please cite this article in press as: T.D. Wilson, et al., Coord. Chem. Rev. (2012), http://dx.doi.org/10.1016/j.ccr.2012.06.015